Received: Added at production | Revised: Added at production | Accepted: Added at production

DOI: xxx/xxxx

RESEARCH ARTICLE

Ground-motion intensity measure correlations observed in Italian strong-motion records

Chen Huang | Carmine Galasso*

[1]Department of Civil, Environmental and Geomatic Engineering, University College London, London, United Kingdom

Correspondence
*Carmine Galasso, Department of Civil, Environmental and Geomatic Engineering, University College London, London, England, UK. Email: c.galasso@ucl.ac.uk

Present Address
Carmine Galasso, Chadwick Building, Gower Street, Room GM14, London WC1E 6BT, United Kingdom

Summary

Ground-motion models (GMMs) are widely used in probabilistic seismic hazard analysis (PSHA) to estimate the probability distributions of earthquake-induced ground-motion intensity measures (IMs) at a site, given an earthquake of a certain magnitude occurring at a nearby location. Accounting for spatial and cross-IM correlations in earthquake-induced ground motions has important implications on probabilistic seismic hazard and loss estimates. This study first develops a new Italian GMM with spatial correlation for 31 amplitude-related IMs, including peak ground acceleration (PGA), peak ground velocity (PGV) and 5% damped elastic pseudo-spectral accelerations (PSAs) at 29 periods ranging from 0.01 s to 4 s. The model estimation is performed through a recently-developed one-stage non-linear regression algorithm proposed by the authors, known as the Scoring estimation approach. In fact, current state-of-practice approaches estimate spatial correlation separately from the GMM estimation, resulting in inconsistent and statistically inefficient estimators of inter- and intraevent variances and parameters in the spatial correlation model. We test whether this affects the subsequent cross-IM correlation analysis. To this aim, based on the newly-developed GMM, the empirical correlation coefficients from inter- and intraevent residuals are investigated. Finally, a set of analytical correlation models between the selected IMs are proposed. This is of special interest as several correlation models between different IMs have been calibrated and validated based on advanced GMMs and global datasets, lacking earthquakes in extensional regions; however, modeling the correlation between different IM types has not been adequately addressed by current, state-of-the-art GMMs and recent ground-motion records for Italy.

KEYWORDS:
intensity measure correlation, ground-motion model, spatial correlation, Italy

1 | INTRODUCTION AND MOTIVATIONS

Ground-motion models (GMMs), also known as ground-motion prediction equations or attenuation relationships, are empirical models describing the probability distributions of intensity measures (IMs) at a site, given an earthquake of a certain magnitude occurring at a nearby location. GMMs are widely used in probabilistic seismic hazard analysis (PSHA). The dependence between

various IMs from a single event at multiple sites plays a crucial role for PSHA of spatially-distributed systems (eg, portfolios of structures and lifelines). Such a dependence is due to common source and wave-traveling paths and to similar distances to fault asperities[1]. Several studies[2,3] have shown that the spatial correlation in ground-motion IMs has important implications on seismic hazard and risk estimates of spatially-distributed engineering systems. Moreover, the cross-IM correlation is often required for the performance-based seismic design and assessment of structures, for instance, in the definition of target IMs to be used for ground-motion simulation, selection, and modification for engineering applications (eg, the generalized conditional intensity measure or GCIM[4]; the conditional spectrum or CS[5]). Both the spatial correlation and the cross-IM correlation can be estimated directly during the GMM estimation stage or indirectly, in a subsequent stage, after the GMM is estimated (see Ming et al[6] for a discussion on this aspect).

Numerous GMMs have been developed based on global, national, and regional datasets and an online GMM compendium has been developed by Douglas[7]. The GMMs applicable to Italy include, but are not limited to, Ambraseys et al[8], Chiou and Youngs[9], Akkar and Bommer[10], Bindi et al[11], Akkar et al[12,13], Chiou and Youngs[14], Lanzano et al[15], respectively (hereafter, referred to as ADSS05, CY08, AB10, ITA10, ASB14, CY14 and ITA18, respectively). The characteristics of these GMMs are summarized in Table 1.

These GMMs are of particular interests in this study for several reasons. In particular, ITA10 is the current state-of-practice GMM for Italy and ITA18 is an updated version of ITA10 (ie, including ground-motion data of recent earthquakes in Italy and some global events in the magnitude range 6.1-8.0). The dataset considered in the present study (introduced in the Section 3) is extracted from the European Strong-Motion (ESM) flatfile[16], which is also the main database used in ITA18. However, unlike ITA18, this study only considered earthquake events occurred in Italy in order to eliminate possible model biases caused by the different geographic and tectonic setting in other regions.

The GMMs discussed above have been applied in several recent PSHA exercises[21]; however, these GMMs have been developed without consideration of the spatial correlation in ground motions, possibly due to the complexity in the estimation process. For instance, Jayaram and Baker[2] developed spatial correlation models for several global earthquakes using the NGA-West (Next Generation of Ground-Motion Attenuation Models for the Western US) GMMs (eg, CY08), proposing a predictive model of the effective range parameter $\widetilde{h}$ (ie, the separation distance between stations at which the spatial correlation is about 0.05) as a function of the structural period T (in seconds). The authors also discussed that the results are insensitive to the choice of the specific GMM. In a similar manner, Esposito and Iervolino[22,23] studied the spatial correlations in Italian and European ground-motion data and developed a set of predictive models for $\widetilde{h}$ using ITA10 and AB10. These predictive models for $\widetilde{h}$[2,23] will be used as the reference studies to compare the results in this study.

Jayaram and Baker[24] and Ming et al[6] have demonstrated that fitting a GMM without spatial correlation to the spatially-correlated data results in an overestimation of the interevent standard deviation (ie, τ, accounting for variability between events) and an underestimation of the intraevent standard deviation (ie, σ, accounting for the variability among observations within an event), although the estimates of the GMM coefficients are consistent in both cases. Since none of the previously introduced GMMs accounts for the spatial correlation and may produce biased inter- and intraevent variances, the subsequent analysis of cross-IM correlation may be (at least in principle) biased too. Thus, it may be important to incorporate the spatial correlation in the GMM estimation stage and in any further analysis involving the use of the developed GMMs.

To incorporate the spatial correlation in the GMM estimation, Jayaram and Baker[24] proposed a multi-stage algorithm adapting conventional geostatistical tools[25]. However, this approach may result in an inconsistent estimation of the parameters in the spatial correlation models, thus, resulting in estimators of the GMM coefficients that, although consistent, are statistically inefficient. Moreover, estimators of τ and σ may be both inconsistent and statistically inefficient. Also, the multi-stage algorithm may suffer from slow convergence and it is sensitive to the initial parameter values. In addition, the multi-stage algorithm cannot account for more advanced (eg, non-stationary) spatial correlation models. The reader can refer to Ming et al[6] for a detailed discussion on those aspects. To address these issues, Ming et al[6] introduced a one-stage algorithm for the estimation of GMMs with spatial correlation, known as the Scoring estimation approach. This method is proved to be statistically rigorous, numerically stable, and capable of estimating various spatial correlation models. The proposed algorithm will be formally introduced in Section 2.

Once a given GMM with spatial correlation has been estimated, it can be used to develop correlation models between different IMs. Several cross-IM correlation models have been calibrated and validated based on the NGA-West and NGA-West2 (Enhancement of Next Generation Attenuation Relationships for Western US) databases and advanced GMMs, including Baker and Jayaram[26], Bradley[27,28], and Baker and Bradley[29] (hereafter, these cross-IM correlation models are referred to as BJ08,

TABLE 1 Characteristics of ground-motion models (GMMs) applicable to Italy

Features	This study	ITA10	ITA18	ADSS05	AB10	ASB14	CY08	CY14
Period∗	1976-2016	1976-2009	1969-2016	1973-2003	1973-2003	1967-2012	1935-2003	1935-2011
Number of earthquakes	233	99	146	135	131	221	125	300
Number of records	7843	769	5607	595	532	1041	1950	12244
Region	Italy	Italy	Italy	Europe and Middle East	Europe and Middle East	Europe and Middle East	Worldwide shallow crustal regions	Worldwide shallow crustal regions
Magnitude range (M_w)	[4.0, 6.9]	[4.1, 6.9]	[3.5, 8.0]	[5.0, 7.6]	[5.0, 7.6]	[4.0, 7.6]	[4.2, 7.9]	[3.1, 7.9]
Distance range (km)†	$R_{JB} \leq 250$	$R_{epi} \leq 200$	$R_{JB} \leq 200$	$R_{JB} \leq 100$	$R_{JB} \leq 100$	$R_{JB} \leq 200$	$R_{rup} \leq 200$	$R_{rup} \leq 400$
Considered IMs	PGA, PGV, PSA($T \leq 4$) (29 periods)]	PGA, PGV, PSA($T \leq 2$) (20 periods)]	PGA, PGV, PSA($T \leq 10$) (36 periods)	PGA, PSA($T \leq 2.5$) (61 periods)	PGA, PSA($T \leq 3$) (60 periods)	PGA, PGV, PSA($T \leq 4$) (62 periods)	PGA, PGV, PSA($T \leq 10$) (22 periods)	PGA, PGV, PSA($T \leq 10$) (24 periods)
IM definition‡	RotD50	Larger	RotD50	Larger	GM	GM	GMRotI50	RotD50
Estimation technique§	Scoring	AY92	lme4	JB93	JB93	AY92	nlme	AY92/JB93

∗Period indicates the time span of the considered dataset;

†R_{JB} is the closest distance to the surface projection of the rupture plane in km; R_{epi} is the epicentral distance in km; R_{rup} is the closest distance to the ruptured fault area in km;

‡'RotD50' is the median orientation-independent non-geometric-mean measure, using period-dependent rotation angle; 'Larger' represents the larger component of the two horizontal components; 'GM' is the geometric mean of the two horizontal components; 'GMRotI50' is the median orientation-independent geometric mean, using period-independent rotation angle.

§'Scoring' is the Scoring estimation approach; AY92 is a one-stage nonlinear mixed-effects algorithm for the estimation of GMM without spatial correlation[17]; JB93 is a one-stage mixed-effects algorithm with linearization for the estimation of GMM without spatial correlation[18]; lme4 is an R package for the estimation of linear mixed-effects models[19]; nlme is an R package for the estimation of nonlinear mixed-effects models[20].

TABLE 2 Characteristics of cross-IM correlation models applicable to Italy

Features	This study	C13	ASA14	BJ08	B11	B12	BB17
Period∗	1976-2016	1973-2003	1967-2012	1935-2003	1935-2003	1935-2003	1935-2011
Number of earthquakes	233	135	221	-	-	-	300
Number of records	7843	595	1041	-	1842	1842	12244
Region	Italy	Europe and Middle East	Europe and Middle East	Worldwide shallow crustal regions	Worldwide shallow crustal regions	Worldwide shallow crustal regions	Worldwide shallow crustal regions
Magnitude range (M_w)	[4.0, 6.9]	[5.0, 7.6]	[4.0, 7.6]	-	[4.2, 7.9]	[4.2, 7.9]	[3.1, 7.9]
Distance range†	$R_{JB} \leq 250$	$R_{JB} \leq 100$	$R_{JB} \leq 200$	-	$R_{rup} \leq 200$	$R_{rup} \leq 200$	$R_{rup} \leq 400$
Cross-IM considered	PSA-PSA, PGA-PSA, PGV-PSA	PSA-PSA	PSA-PSA, PGA-PSA	PSA-PSA	PGA-PSA	PGV-PSA	PSA-PSA, PGA-PSA, PGV-PSA, and others‡
Period range	[0.01, 4]	[0.05, 2.5]	[0.01, 4]	[0.01, 10]	[0.01, 10]	[0.01, 10]	[0.01, 10]
GMM used	This study	ADSS05	ASB14	CY08	CY08 and others§	CY08 and others§	CY14 and others¶
Analytical model (A)/ Table (T) available	A	A	T	A	A	A	T

Period indicates the time span of the considered dataset;

†R_{JB} is the closest distance to the surface projection of the rupture plane in km; R_{epi} is the epicentral distance in km; R_{rup} is the closest distance to the ruptured fault area in km;

‡BB17 has also computed the empirical correlation coefficients between the significant duration between PGA, PGV, and PSA;

§B11 and B12 used other GMMs developed in NGA-West project and then took the average empirical correlations over all considered GMMs;

¶Different GMMs have been used for the significant duration.

B11, B12, and BB17, respectively). In addition, Cimellaro[30] and Akkar et al[31] have studied the cross-IM correlation in European ground-motion data (hereafter, C13 and ASA14). The characteristics of these cross-IM correlation models are presented in Table 2. It is worth noting that Baker and Cornell[32] have observed that the cross-IM correlations are "independent of the ground motion causal magnitudes and distances". However, for the sake of completeness, the magnitude range and distance range of the databases used by the considered studies are also reported in Table 2. These cross-IM correlation models are used as the reference models for comparison in this study. As shown in Table 2, modeling the correlation between different IM types has not been adequately addressed by current, state-of-the-art ground-motion models for Italy. As discussed by Scasserra et al[33], Italian data is of special interest because (1) it is principally from earthquakes in extensional regions that are poorly represented in global databases, and (2) past practice in Italy has used local GMMs based on limited datasets that cannot resolve many significant source, path, and site effects. Kotha et al[34] have recently quantified the regional differences in the apparent attenuation of high frequency ground motions with distance between three groups of strong-motion records: (1) Italy; (2) Turkey, and (3) rest of the Europe-Middle-East region. The authors argue that, although a regionalization based on the tectonic settings could be more appropriate to explore regional differences in ground motion, a country-based categorization can reflect much better the data availability and the unbalanced composition of various dataset around Europe. Boore et al[35] have stressed that country names are often used in GMMs as a convenient shorthand to describe regions, realizing that results for the region may well be applicable beyond the political boundaries of the country and that regional differences of attenuation may occur within the countries. This also applies to the study presented here. It is usually difficult to obtain enough data to establish the geographic limits of a given GMM nor to parse the data more finely.

To properly study the cross-IM correlations in Italian strong-motion records, this study first develops a new Italian GMM with spatial correlation for various amplitude-based IMs. The model estimation is performed through the Scoring estimation approach recently proposed by the authors. Based on the newly-developed GMM, this study finally proposes a set of empirical and analytical correlation models between the selected IMs for Italy.

2 | METHODOLOGY

2.1 | Model specification

A typical GMM is presented as a mixed-effect nonlinear model with a certain spatial correlation structure[24] and it can be written in a vector form as in equation (1),

$$\mathbf{Y}_i = \mathbf{f}(\mathbf{X}_i, \mathbf{b}) + \boldsymbol{\eta}_i + \boldsymbol{\varepsilon}_i\,, \quad i = 1, \dots, N\,, \tag{1}$$

where:

- $\mathbf{Y}_i = \log \mathbf{IM}_i = \left(\log \mathrm{IM}_{i1}, \dots, \log \mathrm{IM}_{ij}, \dots, \log \mathrm{IM}_{in_i}\right)^\top$ is an $n_i \times 1$ vector of logarithmic[1] IMs of interest at all sites $j \in \{1, \dots, n_i\}$ during earthquake i;
- $\mathbf{f}(\mathbf{X}_i, \mathbf{b}) = \left(f(\mathbf{X}_{i1}, \mathbf{b}), \dots, f(\mathbf{X}_{in_i}, \mathbf{b})\right)^\top$ is an $n_i \times 1$ vector of ground-motion prediction functions $f(\mathbf{X}_{ij}, \mathbf{b})$ at all sites $j \in \{1, \dots, n_i\}$ during earthquake i;
- $\mathbf{X}_{ij}$ represents a vector of predictors (eg, magnitude, source-to-site distance, soil type at site) for site j during earthquake i;
- $\mathbf{b} \in \mathbb{R}^p$ is a $p \times 1$ vector of unknown model parameters;
- $\boldsymbol{\eta}_i = \eta_i \mathbf{1}_{n_i}$ for all $i \in \{1, \dots, N\}$ and $(\eta_i)_{i=1,\dots,N}$ are independent and identically distributed inter-event errors with $\mathbb{E}(\eta_i) = 0$ and $\mathrm{var}(\eta_i) = \tau^2$ for all $i \in \{1, \dots, N\}$, where $\mathbf{1}_{n_i}$ is an $n_i \times 1$ vector of ones;
- $(\boldsymbol{\varepsilon}_i)_{i=1,\dots,N}$ are independent intra-event error vectors of size $n_i \times 1$ with $\mathbb{E}(\boldsymbol{\varepsilon}_i) = \mathbf{0}$ and $\mathrm{cov}(\boldsymbol{\varepsilon}_i) = \sigma^2 \boldsymbol{\Omega}_i(\boldsymbol{\omega})$, where $\boldsymbol{\Omega}_i(\boldsymbol{\omega})$ is the correlation matrix corresponding to earthquake i with $\boldsymbol{\omega}$, a vector of unknown parameters;
- $(\eta_i)_{i=1,\dots,N}$ and $(\boldsymbol{\varepsilon}_i)_{i=1,\dots,N}$ are assumed to be mutually independent;
- N is the total number of earthquakes;

[1] It is worth noting that both the decadic logarithm (base 10) and the natural logarithm (base e) are used in common GMMs. However, this choice does not affect the model assumptions.

- n_i is the number of recording stations during earthquake i.

For consistency with Ming et al[6], the functional form of $f(\mathbf{X}_{ij}, \mathbf{b})$ is the same as AB10 in equation (2), which can regarded as a simplified function of ITA10,

$$f(\mathbf{X}_{ij}, \mathbf{b}) = b_1 + b_2\, M_i + b_3\, M_i^2 + (b_4 + b_5\, M_i) \log_{10}\left(\sqrt{R_{JB,ij}^2 + b_6^2}\right) + b_7\, S_{S,j} + b_8\, S_{A,j} + b_9\, F_{N,i} + b_{10}\, F_{R,i}\,, \tag{2}$$

where

- M_i is the moment magnitude (M_w) of event i;
- $R_{JB,ij}$ is the Joyner-Boore distance in kilometers at station j during event i;
- $S_{S,j}$ and $S_{A,j}$ are dummy variables determining the soil type at station j according to

$$(S_{S,j},\, S_{A,j}) = \begin{cases} (1,\, 0)\,, & \text{soft soil,} \\ (0,\, 1)\,, & \text{stiff soil,} \\ (0,\, 0)\,, & \text{rock;} \end{cases} \tag{3}$$

- $F_{N,i}$ and $F_{R,i}$ are dummy variables indicating the style-of-faulting of earthquake i according to

$$(F_{N,i},\, F_{R,i}) = \begin{cases} (1,\, 0)\,, & \text{normal fault,} \\ (0,\, 1)\,, & \text{reverse fault,} \\ (0,\, 0)\,, & \text{strike-slip fault.} \end{cases} \tag{4}$$

It is worth noting that the focus of this study is on investigating the ground-motion intensity measure correlations observed in Italian data. Hence, a fairly simple ground-motion prediction function, $f(\mathbf{X}_{ij}, \mathbf{b})$, has been selected for this purpose. As discussed in Baker and Cornell[32] and Baker and Jayaram[26], the choice of a particular GMM functional form has an almost negligible effect on the correlation estimates.

To take the spatial correlation into account, the jj'-th entry, $\boldsymbol{\Omega}_{i,jj'}(\boldsymbol{\omega})$, of $\boldsymbol{\Omega}_i(\boldsymbol{\omega})$ is specified as

$$\boldsymbol{\Omega}_{i,jj'}(\boldsymbol{\omega}) = k(\mathbf{s}_{ij},\, \mathbf{s}_{ij'}) = \rho(\varepsilon_{ij}, \varepsilon_{ij'}) \tag{5}$$

for all $i \in \{1, \dots, N\}$ and $j, j' \in \{1, \dots, n_i\}$, where $k(\mathbf{s}_{ij},\, \mathbf{s}_{ij'})$ gives the correlation $\rho(\varepsilon_{ij},\, \varepsilon_{ij'})$ between ε_{ij} and $\varepsilon_{ij'}$ at locations $\mathbf{s}_{ij}$ and $\mathbf{s}_{ij'}$ of sites j and j' during earthquake i.

There are many options for correlation functions available in the literature[36]. For spatially independent intra-event errors (ie, no spatial correlation is modeled),

$$k(\mathbf{s}_{ij},\, \mathbf{s}_{ij'}) = 0, \tag{6}$$

for all sites $j \neq j'$ during earthquake i. For stationary and isotropic process of intra-event errors, the correlation $\rho(\varepsilon_{ij},\, \varepsilon_{ij'})$ only depends on $d_{i,jj'} = \|\mathbf{s}_{ij} - \mathbf{s}_{ij'}\|_2$, the Euclidean distance between sites j and j' during earthquake i, such that

$$k(\mathbf{s}_{ij},\, \mathbf{s}_{ij'}) = k(d_{i,jj'})\,. \tag{7}$$

One of the common choices of this type of correlation functions is the exponential model[2,22,23],

$$k(d) = \exp\left(-\frac{d}{h}\right) \tag{8}$$

where h is a positive range parameter in kilometres, at which the spatial correlation is around 0.37. It is worth noting that equation (8) is slightly different from the one used by Jayaram and Baker[2] and Esposito and Iervolino[22,23], which is

$$k(d) = \exp\left(-\frac{3d}{\widetilde{h}}\right)\,, \tag{9}$$

where $\widetilde{h}$ is the effective range[25], the distance at which the spatial correlation is around 0.05. The relationship between the effective range $\widetilde{h}$ and the range parameter h is

$$\widetilde{h} = 3h\,. \tag{10}$$

The GMM is developed for 31 amplitude-based IMs, including, peak ground acceleration (PGA) in cm/s^2, peak ground velocity (PGV) in cm/s, and 5% damped elastic pseudo-spectral accelerations (PSAs) at 29 periods ranging from 0.01 s to 4 s in cm/s^2. The RotD50 IM definition of horizontal components[37] is used in this study, consisting of the median single-component

horizontal ground motion across all non-redundant azimuths. As shown in Table 1, various IM definitions are used in the literature, however, the difference among them is fairly small[37,38].

2.2 | Estimation algorithm

The Scoring estimation approach, which is a modified Newton-Raphson algorithm, is briefly described here. Details can be found in Ming et al[6]. The unknown parameters in the GMM, $\boldsymbol{\alpha} = (\mathbf{b}^\top, \boldsymbol{\theta}^\top)^\top$ as the complete vector of model parameters, where $\boldsymbol{\theta} = (\tau^2, \sigma^2, \boldsymbol{\omega}^\top)^\top$ with $\boldsymbol{\omega}$ being a vector of the parameters in the spatial correlation function (eg, h in equation [8]), are estimated by maximizing the log-likelihood function, $l(\boldsymbol{\alpha})$, as follows:

$$l(\boldsymbol{\alpha}) = -\frac{\sum_{i=1}^{N} n_i}{2}\ln(2\pi) - \frac{1}{2}\ln|\mathbf{C}(\boldsymbol{\theta})| - \frac{1}{2}[\mathbf{Y} - \mathbf{f}(\mathbf{X}, \mathbf{b})]^\top \mathbf{C}^{-1}(\boldsymbol{\theta})[\mathbf{Y} - \mathbf{f}(\mathbf{X}, \mathbf{b})] \tag{11}$$

where $\mathbf{Y} = (\mathbf{Y}_1^\top, \cdots, \mathbf{Y}_N^\top)^\top$; $\mathbf{f}(\mathbf{X}, \mathbf{b}) = \left(\mathbf{f}(\mathbf{X}_1, \mathbf{b})^\top, \cdots, \mathbf{f}(\mathbf{X}_N, \mathbf{b})^\top\right)^\top$; covariance matrix $\mathbf{C}(\boldsymbol{\theta})$ is a block diagonal matrix of $\mathbf{C}_i$, where $\mathbf{C}_i = \tau^2 \mathbf{1}_{n_i \times n_i} + \sigma^2 \boldsymbol{\Omega}_i(\boldsymbol{\omega})$.

The Scoring estimation approach finds the estimate of $\boldsymbol{\alpha}$ that maximizes $l(\boldsymbol{\alpha})$ in equation (11) via the general updating equation (12):

$$\widehat{\boldsymbol{\alpha}}^{(k+1)} = \widehat{\boldsymbol{\alpha}}^{(k)} + \mathbf{I}^{-1}(\widehat{\boldsymbol{\alpha}}^{(k)})\mathbf{S}(\widehat{\boldsymbol{\alpha}}^{(k)}) \tag{12}$$

where $\widehat{\boldsymbol{\alpha}}^{(k)}$ denotes the estimate of $\boldsymbol{\alpha}$ at iteration step k , and

$$\mathbf{S}(\boldsymbol{\alpha}) = \frac{\partial l(\boldsymbol{\alpha})}{\partial \boldsymbol{\alpha}} \quad \text{and} \quad \mathbf{I}(\boldsymbol{\alpha}) = \mathbb{E}\left[\frac{\partial l(\boldsymbol{\alpha})}{\partial \boldsymbol{\alpha}} \frac{\partial l(\boldsymbol{\alpha})}{\partial \boldsymbol{\alpha}^\top}\right] . \tag{13}$$

The updating equation for the Scoring estimation approach are obtained by replacing the negative Hessian matrix in the Newton-Raphson algorithm, $-\mathbf{H}(\boldsymbol{\alpha})$, by the Fisher information matrix, $\mathbf{I}(\boldsymbol{\alpha})$ [39].

In summary, the steps of the Scoring estimation approach are as follows:

1. Set initial values $\boldsymbol{\alpha}^{(1)}$;
2. Update the estimates of $\boldsymbol{\alpha}$ by equation (12);
3. Repeat step 2 until the log-likelihood function in equation (11) is maximized and the estimates for the parameters converge.

2.3 | Computation of cross-IM correlation

Once the GMM with spatial correlation has been estimated, the cross-IM correlation can be estimated by the empirical Pearson correlation coefficients. The same method is used by the considered studies in Table 2. This study have applied the following steps to compute the empirical correlation coefficients:

1. Compute the inter- and intra-event residuals for each IM,

$$\widehat{\eta}_i = \frac{\frac{1}{\widehat{\sigma}^2}\mathbf{1}_{n_i}^\top \boldsymbol{\Omega}_i^{-1}(\widehat{\boldsymbol{\omega}})[\mathbf{Y}_i - \mathbf{f}(\mathbf{X}_i, \widehat{\mathbf{b}})]}{\frac{1}{\widehat{\tau}^2} + \frac{1}{\widehat{\sigma}^2}\mathbf{1}_{n_i}^\top \boldsymbol{\Omega}_i^{-1}(\widehat{\boldsymbol{\omega}})\mathbf{1}_{n_i}} \quad , \quad \widehat{\boldsymbol{\varepsilon}}_i = \mathbf{Y}_i - \mathbf{f}(\mathbf{X}_i, \widehat{\mathbf{b}}) - \widehat{\eta}_i \mathbf{1}_{n_i} ; \tag{14}$$

2. Scale the residuals by the estimated standard deviations from the proposed GMM with spatial correlation,

$$\widetilde{\eta}_i = \frac{\widehat{\eta}_i}{\widehat{\tau}} , \ \widetilde{\boldsymbol{\varepsilon}}_i = \frac{\widehat{\boldsymbol{\varepsilon}}_i}{\widehat{\sigma}} ; \tag{15}$$

3. Compute the empirical correlation coefficient, as follows,

$$\rho(\mathrm{IM}_1, \mathrm{IM}_2) = \frac{\rho(\widetilde{\boldsymbol{\eta}}^{(1)}, \widetilde{\boldsymbol{\eta}}^{(2)})\widehat{\tau}^{(1)}\widehat{\tau}^{(2)} + \rho(\widetilde{\boldsymbol{\varepsilon}}^{(1)}, \widetilde{\boldsymbol{\varepsilon}}^{(2)})\widehat{\sigma}^{(1)}\widehat{\sigma}^{(2)}}{\sigma_{\text{total}}^{(1)}\sigma_{\text{total}}^{(2)}} , \tag{16}$$

where $\rho(\widetilde{\boldsymbol{\eta}}^{(1)}, \widetilde{\boldsymbol{\eta}}^{(2)})$ and $\rho(\widetilde{\boldsymbol{\varepsilon}}^{(1)}, \widetilde{\boldsymbol{\varepsilon}}^{(2)})$ are the correlation coefficients of the inter- and intra-event residuals of a pair of IMs of interest (ie, IM_1 and IM_2), respectively; $\sigma_{total} = \sqrt{\widehat{\sigma}^2 + \widehat{\tau}^2}$.

2.4 | Modeling of cross-IM correlation

Following Baker and Cornell[32], the analytical correlation model between various IMs is developed through the following steps:

1. Apply the Fisher z transformation to the empirical correlation coefficients, as follows,
$$z = \frac{1}{2}\ln\left(\frac{1+\rho}{1-\rho}\right), \tag{17}$$
where z is the transformed data with a constant variance, $\mathrm{Var}(z) = 1/\sqrt{\sum_{i=1}^{N} n_i - 3}$;
2. Propose a parametric correlation model $\rho(\boldsymbol{\phi})$;
3. Estimate the parameters $\boldsymbol{\phi}$ by nonlinear least squares and the objective function is
$$\min_{\boldsymbol{\phi}} \sum_{i=1}^{K}\sum_{j=1}^{K}\left(z_{ij} - \frac{1}{2}\ln\left(\frac{1+\rho_{ij}(\boldsymbol{\phi})}{1-\rho_{ij}(\boldsymbol{\phi})}\right)\right)^2, \tag{18}$$
where K is the number of IMs considered.

Although the current practice estimates the GMM for each IM individually and then assess the cross-IM correlation coefficients/models separately, several studies[40,41] have shown that it is possible but challenging to incorporate the spatial cross-IM (ie, considering both spatial correlation and cross-IM correlation at the same time) in the GMM estimation process, requiring often stricter assumptions. The developed one-stage estimation approach can also account for the cross-IM correlation and this feature is currently under investigation by the authors, especially in terms of implications on the GMM estimates.

3 | GROUND-MOTION DATABASE

As briefly mentioned in the previous section, the considered dataset is extracted from the ESM flatfile[16] and the following selection criteria are applied,

- events occurred within Italy, with moment magnitude $M_w \geq 4$ and with at least two recording sites are considered;
- recording stations with Joyner-Boore distance[2] (ie, the closest distance to the surface projection of the rupture plane) $R_{JB} \leq 250$ km are considered;
- recording stations are free-field;
- records without information of M_w, fault types, or V_{S30} (ie, the average shear-wave velocity in the upper 30 m of the soil) are removed;
- recording stations with redundant site information (eg, co-located sites) are removed.

The final dataset includes 7843 records from 233 earthquakes in the magnitude range $4 \leq M_w \leq 6.9$ in Italy from 1976 to 2016. The geographical distribution of the selected dataset is shown in Figure 1, together with the $M_w - R_{JB}$ distribution and the site classifications of selected data according to Eurocode 8[43]. 66% of the selected ground-motion records are caused by the rupture of normal faults, 23% of the selected ground-motion records are caused by reverse faults and 11% of the records are caused by strike-slip faults. Most data is collected from stations of site class B/stiff soil and the median V_{S30} across stations is about 637 m/s.

4 | RESULTS AND DISCUSSIONS

4.1 | GMM with spatial correlation

The estimated parameters of the proposed GMM with spatial correlation are presented in Table 3. For illustrative purposes, the median predictions for PGA, PGV, PSA(T=1.0), and PSA spectra are shown in Figure 2, in comparison with the GMMs in

[2]If the finite-fault model is available, R_{JB} is computed based on the fault geometry by ESM; if not, for $M_w > 5.5$, R_{JB} is estimated from epicenter distance R_{epi} by empirical correlation[42], otherwise the earthquake source is assumed to be a point source and $R_{JB} = R_{epi}$.

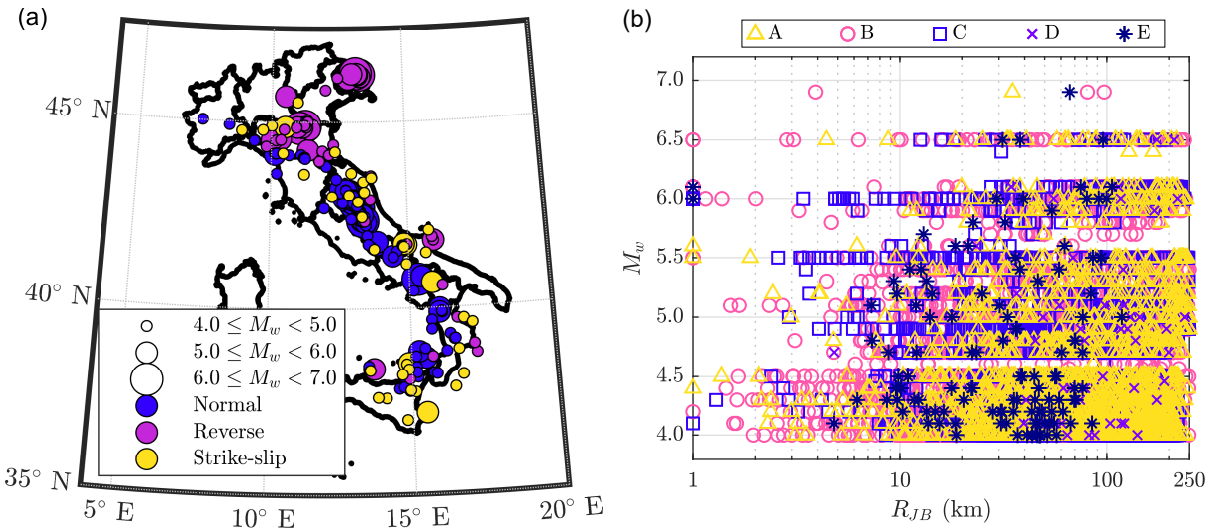

FIGURE 1 (a) Geographical distribution of considered earthquakes, classified according to focal mechanisms; (b) M_w-R_{JB} distribution with the Eurocode 8 site classification. The color version of this figure is available only in the electronic edition.

Table 1, for stiff soil assuming $V_{S30} = 580$ m/s for a M_w 5.5 normal fault event[3]. The observations of normal fault events with magnitude M_w 5.5 $\pm$ 0.3 are also presented to assess the general performance of the considered GMMs.

It is shown that the proposed GMM for PGA, PGV, and spectral ordinates is generally consistent with the reference GMMs and are in line with the observations, as the reference GMMs and the observed data generally lie within $\pm 1\,\sigma_{total}$ of the derived models. As discussed earlier, the incorporation of spatial correlation has little impact on the estimate of **b** and the considered GMMs are expected to have consistent median predictions. Moreover, the obtained results also confirm the faster attenuation of Italian strong ground-motion data compared to the global data, as also observed in Scasserra et al[33] and Zimmaro et al[44].

However, the incorporation of spatial correlation, in comparison with the model estimated without spatial correlation, results in a reduction of the interevent variance and an increase of the intraevent variance. The estimated parameters and the corresponding 95% confidence interval (CI) of GMMs with and without spatial correlations for PGA, PGV, and PSA($T = 1$s) derived in this study are presented in Table 4, which confirms this statement and the same conclusions hold for all the other IMs.

To compare the performances of the GMMs with and without spatial correlation, the Akaike Information Criteria (AIC)[45] and the Bayesian Information Criteria (BIC)[46], which deal with the trade-off between the goodness of fit of the model and the simplicity of the model (ie, whether or not to include the spatial correlation), are reported in Table 4. The model with lower AIC or BIC value would be the preferred one. It is shown that the GMM with spatial correlation has about 10% lower AIC and BIC than the GMM without spatial correlation, implying that the GMM with spatial correlation model provides a better representation of the considered dataset over those without spatial correlation.

Furthermore, it is also shown in Table 4 whether the estimated parameters are significantly different from zeros assuming a 5% significance level (ie, whether zero is included within the 95% CI). The range parameter h is significantly different from zero as its 95% CI does not include zero, which implies that the spatial correlation is a non-negligible feature of ground motions. However, the parameters b_2 and b_3 for magnitude scaling and b_9 and b_{10} for style-of-faulting scaling may be zeros (ie, these terms may not be significant in capturing the ground-motion features), since the null hypothesis that these parameters equal to zeros cannot be rejected assuming a 5% significance level. These findings are consistent with the observations in Bommer et al[47] and Lanzano et al[15]. However, these results do not mean that these physical parameters are not important in the GMM but, rather, they imply that the functional form involving these parameters is not a good representation of that feature. Lanzano et al[15] have suggested that the failure to reject null hypothesis regarding the magnitude scaling may be because the large variability in magnitude scaling and uncertainty in the estimation of some predefined parameters (eg, M_h hinge magnitude in ITA18).

[3] M_w is set to 5.5, which is the median of the applicable magnitude range of this study; for CY08 and CY14, the rake angle is set to -90° and dip angle is set to 0° to represent normal fault geometry, no aftershock/hanging-wall effect/basin effect is considered.

TABLE 3 Estimated parameters for the ground-motion models proposed in this study

IM	b_1	b_2	b_3	b_4	b_5	b_6	b_7	b_8	b_9	b_{10}	τ	σ	h (km)
PGA	3.524	0.247	-0.020	-3.936	0.351	12.417	0.228	0.160	-0.060	0.080	0.247	0.370	8.476
PGV	0.742	0.188	0.015	-3.089	0.286	8.529	0.308	0.144	-0.021	0.037	0.261	0.301	3.788
0.010	3.544	0.244	-0.019	-3.943	0.352	12.438	0.228	0.160	-0.060	0.080	0.247	0.370	8.333
0.025	3.770	0.191	-0.016	-3.995	0.359	12.220	0.224	0.156	-0.059	0.082	0.248	0.372	7.730
0.040	4.340	0.099	-0.014	-4.198	0.387	11.956	0.212	0.148	-0.054	0.091	0.249	0.385	7.596
0.050	4.668	0.048	-0.013	-4.303	0.399	11.931	0.211	0.155	-0.055	0.096	0.243	0.401	9.919
0.070	4.975	0.034	-0.013	-4.401	0.404	12.404	0.215	0.157	-0.070	0.092	0.237	0.420	12.964
0.100	4.941	0.099	-0.015	-4.345	0.379	14.067	0.212	0.163	-0.088	0.090	0.244	0.430	12.816
0.150	3.667	0.445	-0.032	-3.867	0.290	15.633	0.192	0.160	-0.087	0.099	0.248	0.416	9.761
0.200	2.584	0.687	-0.042	-3.454	0.225	16.378	0.190	0.162	-0.088	0.094	0.251	0.394	6.343
0.250	1.710	0.793	-0.039	-3.011	0.165	15.061	0.195	0.132	-0.076	0.083	0.260	0.366	2.080
0.300	1.214	0.808	-0.034	-2.748	0.137	13.969	0.220	0.140	-0.076	0.059	0.257	0.357	2.396
0.350	0.867	0.802	-0.026	-2.538	0.109	13.637	0.246	0.141	-0.071	0.048	0.255	0.346	1.927
0.400	0.573	0.786	-0.019	-2.387	0.096	12.917	0.260	0.138	-0.068	0.042	0.258	0.337	1.360
0.450	0.170	0.834	-0.021	-2.274	0.090	12.086	0.280	0.146	-0.068	0.031	0.261	0.333	1.375
0.500	-0.131	0.861	-0.020	-2.174	0.081	11.509	0.293	0.149	-0.069	0.025	0.265	0.329	1.405
0.600	-0.481	0.838	-0.012	-2.020	0.068	10.626	0.312	0.151	-0.053	0.015	0.269	0.324	2.227
0.700	-0.648	0.764	-0.002	-1.913	0.066	9.487	0.319	0.153	-0.038	0.010	0.276	0.316	2.922
0.750	-0.844	0.785	-0.002	-1.869	0.063	9.292	0.323	0.152	-0.032	0.006	0.278	0.314	3.375
0.800	-0.884	0.753	0.002	-1.850	0.066	8.990	0.326	0.151	-0.031	-0.001	0.281	0.312	3.823
0.900	-1.235	0.798	0.000	-1.786	0.064	8.238	0.331	0.145	-0.024	-0.007	0.286	0.310	3.682
1.000	-1.329	0.754	0.006	-1.753	0.068	7.660	0.343	0.144	-0.013	-0.006	0.291	0.307	3.877
1.200	-1.602	0.744	0.008	-1.720	0.076	7.043	0.355	0.143	-0.002	-0.017	0.298	0.305	4.463
1.400	-1.827	0.726	0.013	-1.670	0.077	6.393	0.356	0.137	0.004	-0.020	0.301	0.303	5.485
1.600	-1.869	0.684	0.016	-1.714	0.091	6.070	0.365	0.133	0.008	-0.022	0.304	0.300	5.599
1.800	-1.782	0.580	0.029	-1.692	0.089	5.903	0.358	0.129	0.011	-0.026	0.306	0.300	6.547
2.000	-1.887	0.572	0.030	-1.689	0.091	5.858	0.345	0.127	0.021	-0.020	0.308	0.299	7.921
2.500	-2.114	0.596	0.026	-1.785	0.114	5.873	0.324	0.115	0.042	-0.014	0.320	0.298	9.095
3.000	-2.113	0.531	0.032	-1.822	0.122	6.108	0.314	0.112	0.061	-0.017	0.330	0.298	8.906
3.500	-2.166	0.500	0.035	-1.843	0.126	6.275	0.304	0.101	0.081	-0.010	0.337	0.298	9.585
4.000	-2.088	0.438	0.039	-1.914	0.141	6.361	0.305	0.101	0.094	0.000	0.340	0.301	9.688

Regarding the style-of-faulting scaling, the failure to reject null hypothesis may be because of the limited difference between amplitudes of motions from normal faulting earthquakes (the majority in the considered dataset), with respect to those from strike-slip events[47]. However, it is decided here to keep the functional form as in equation (2), although some parameters may have limited impact on model performance.

An illustrative example of residual analysis is shown in Figure 3, in which the interevent residuals are presented with respect to magnitude and the intraevent residuals with respect to distance. It is shown that there is no major bias in the residuals with respect to distance or magnitude, which implies an overall good fitting of the derived models to the Italian data.

The parameters in the spatial correlation are estimated by the Scoring estimation approach developed by the authors as a by-product of the GMM estimation and are reported in Table 3. To compare the results with existing studies, the effective range $\widetilde{h}$ computed from h (ie, equation [10]) is compared to the predictive models of Jayaram and Baker[2] for cluster site scenario (ie, V_{S30} values show that there are clusters of sites in which the geologic conditions of the soil are similar) and the model of Esposito and Iervolino[23] for Italy, as shown in Figure 4. It is shown that the overall trend of $\widetilde{h}$ obtained in this study is consistent with the two reference models. However, the effective range $\widetilde{h}$ derived in this study is generally smaller than the reference models.

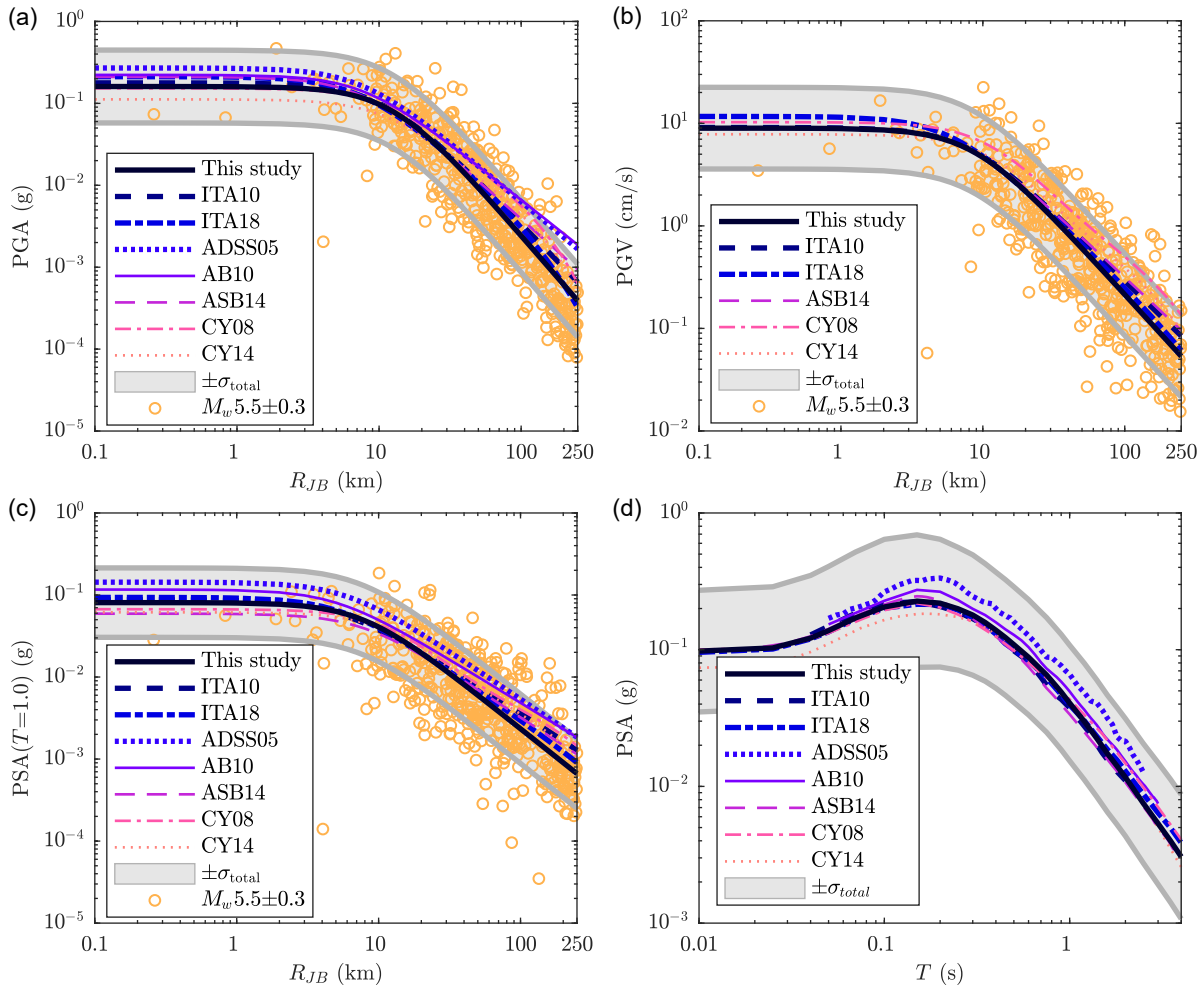

FIGURE 2 Median predictions for (a) PGA, (b) PGV, (c) PSA(T=1.0), and (d) PSA spectra in comparison with existing GMMs for Italy, for stiff soil assuming V_{S30} = 580 m/s for a M_w 5.5 normal fault event. The color version of this figure is available only in the electronic edition.

This may be due to the use of the classical geostatistical method, which generally tends to overestimate the parameters in spatial correlation[6].

It is worth pointing out that, in addition to the inclusion of spatial correlation, other factors also have impacts on the estimations of interevent and intraevent variances, such as, model assumptions, functional forms, estimation algorithms, and dataset etc. As shown in Figure 5, the inter- and intraevent standard deviations (in $\log_{10}$ unit) are slightly higher than the considered studies. This study takes into account a larger number of events among most of the considered study as shown in Table 1 while the functional form is simple compared to the other studies, as discussed above. Thus, the inter-event variance is slightly higher than others. Regarding the intraevent variance, as expected, the inclusion of spatial correlation increases the intraevent variance compared to models without spatial correlation. In general, the total standard deviations in this study are slightly higher than the considered study, which may be partially due to the inclusion of spatial correlation and partially because of the larger dataset used in this study.

4.2 | The empirical correlation coefficient

The contours of the empirical PSA correlation coefficients as a function of T_1 and T_2 (ie, period pairs ranging 0.01 s and 4 s) are shown in Figure 6, which are compared to the cross-IM correlation models listed in Table 2. The empirical correlation coefficients are also available in Table A1 to A3 in Appendix. The visual comparison of Figure 6 shows that the general trends

TABLE 4 Estimated parameters for PGA, PGV, PSA(T=1) GMM with and without spatial correlation (denoted by S and NS)

α	PGA				PGV				PSA(T = 1s)			
	S	±CI†	NS	±CI	S	±CI	NS	±CI	S	±CI	NS	±CI
b_1	3.524	2.188	3.429	2.242	0.742	2.174	0.621	2.197	-1.329	2.384	-1.275	2.411
b_2	0.247	0.868	0.292	0.894	0.188	0.871	0.205	0.881	0.754	0.962	0.715	0.976
b_3	-0.020	0.087	-0.021	0.090	0.015	0.087	0.017	0.088	0.006	0.096	0.011	0.098
b_4	-3.936	0.307	-3.878	0.315	-3.089	0.239	-2.993	0.250	-1.753	0.178	-1.693	0.158
b_5	0.351	0.056	0.333	0.043	0.286	0.037	0.268	0.032	0.068	0.034	0.059	0.030
b_6	12.417	1.176	12.789	0.868	8.529	0.875	8.158	0.722	7.660	1.019	7.215	0.836
b_7	0.228	0.026	0.202	0.026	0.308	0.023	0.304	0.023	0.343	0.023	0.333	0.023
b_8	0.160	0.014	0.110	0.017	0.144	0.013	0.122	0.015	0.144	0.014	0.119	0.015
b_9	-0.060	0.097	-0.058	0.100	-0.021	0.098	-0.026	0.099	-0.013	0.108	-0.024	0.109
b_{10}	0.080	0.113	0.076	0.117	0.037	0.114	0.035	0.116	-0.006	0.126	-0.013	0.127
τ^2	0.061	0.014	0.070	0.015	0.068	0.014	0.071	0.014	0.085	0.017	0.089	0.018
σ^2	0.137	0.005	0.119	0.004	0.090	0.003	0.086	0.003	0.094	0.003	0.090	0.003
h	8.476	0.600	-	-	3.788	0.384	-	-	3.877	0.389	-	-
AIC	5601	-	6169	-	3356	-	3665	-	3680	-	4089	-
BIC	5692	-	6253	-	3447	-	3749	-	3771	-	4173	-

†CI: confidence interval.

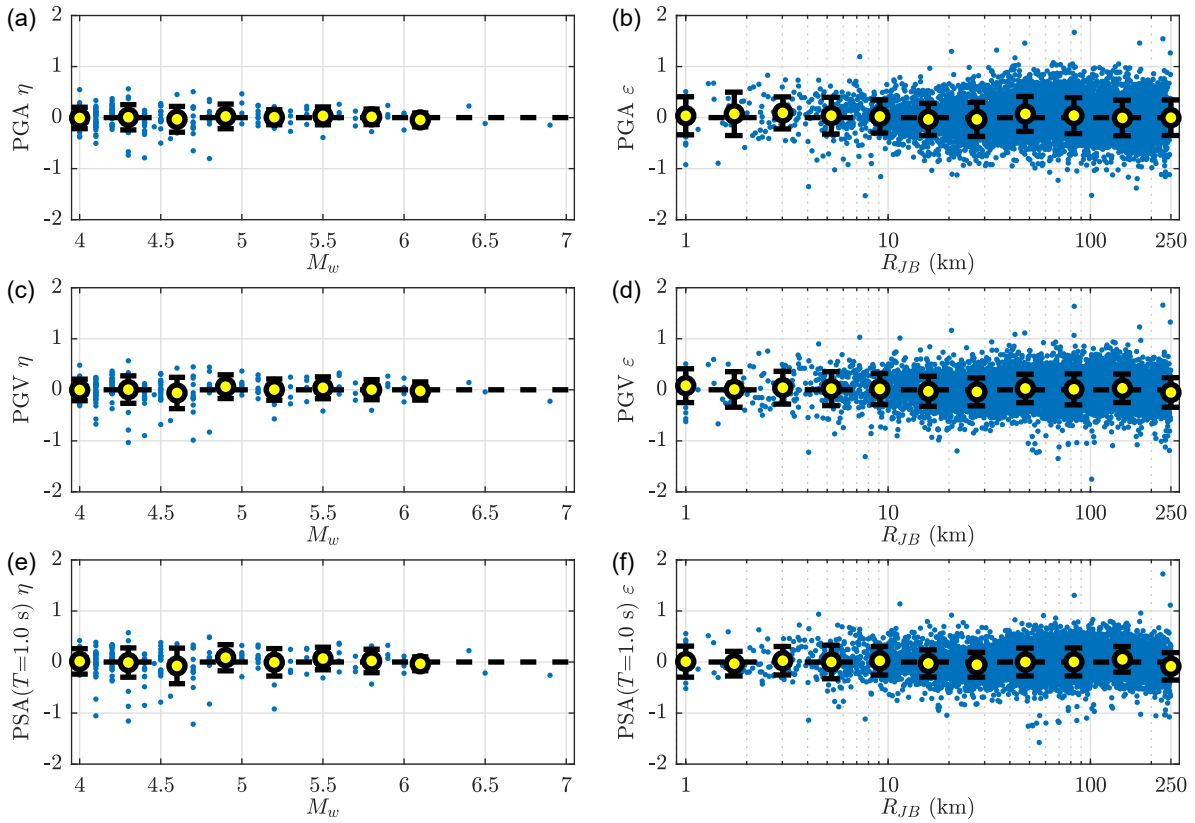

FIGURE 3 *Left*: Interevent residuals versus magnitude. Right: Intraevent residuals versus distance. (a)(b) for PGA, (c)(d) for PGV, (e)(f) for PSA(T=1.0). The color version of this figure is available only in the electronic edition.

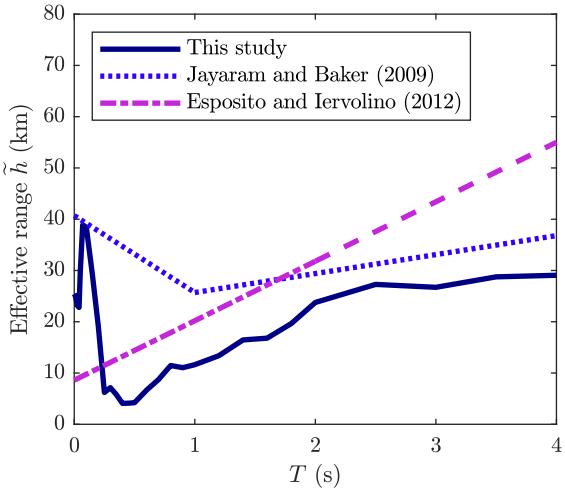

FIGURE 4 Comparison of the effective range $\widetilde{h}$ observed in this study with the models of Jayaram and Baker[2] and Esposito and Iervolino[23]. The dashed line represents the extrapolation of Esposito and Iervolino[23] model. The color version of this figure is available only in the electronic edition.

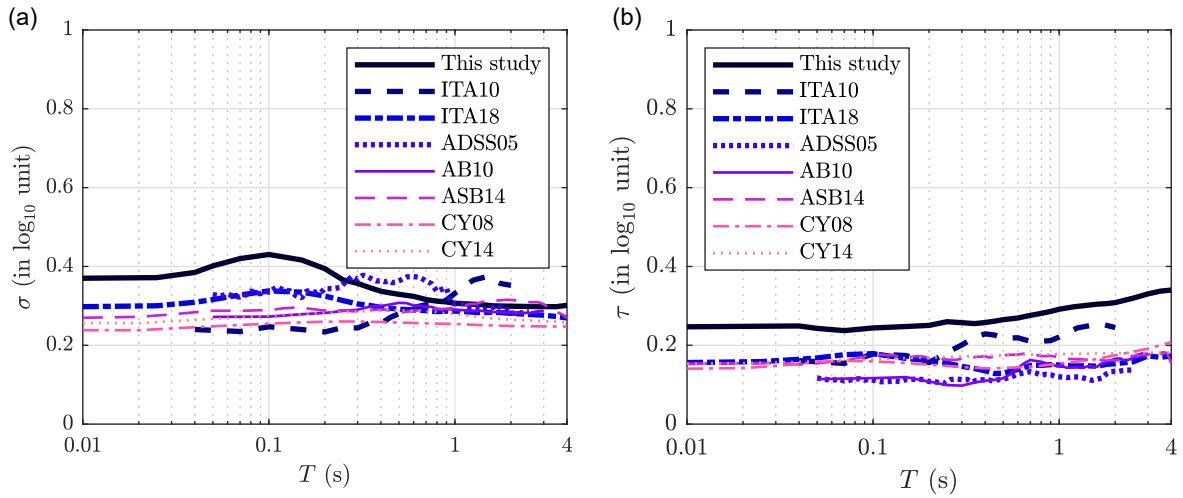

FIGURE 5 (a) Intra-event standard deviation σ; (b) Inter-event standard deviation τ. The color version of this figure is available only in the electronic edition.

of PSA correlation observed in this study are similar to the considered studies, although some differences can be observed when $|T_1 - T_2|$ is large.

Figure 7 shows the empirical correlation coefficients of PSA at two representative periods (ie, $T_2 = 0.1$ s and 1.0 s) versus T_1 ranging from 0.01 s and 4 s. It is shown that the C13 model is significantly different from the other three models and may produce negative correlations for some period pairs, which may "have a numerical error" according to Baker and Bradley[29]. Compared to the worldwide models (excluding the C13 model), there is higher PSA correlation observed in the Italian data, particularly, when the separation between T_1 and T_2 is large (eg, 0.01 s and 4 s). The observed difference may be because the extensional (normal fault) earthquakes are not well represented in the dataset used by the considered studies. Over 66% ground-motion data used in this study are caused by the rupture of normal faults in Italy. In the contrast, the NGA-West database has only about 5% records from events caused by the normal fault rupture[48], the RESORCE dataset used by ASB14 has around 31% records of normal faults[49], and the dataset used in C13[30] has about 32% records corresponding to normal fault events (estimated from the graph). These results may imply that the correlations observed in Italian data have special features which are not well captured by the considered studies. Moreover, Figure 7 also shows that the difference between the empirical correlation coefficients of

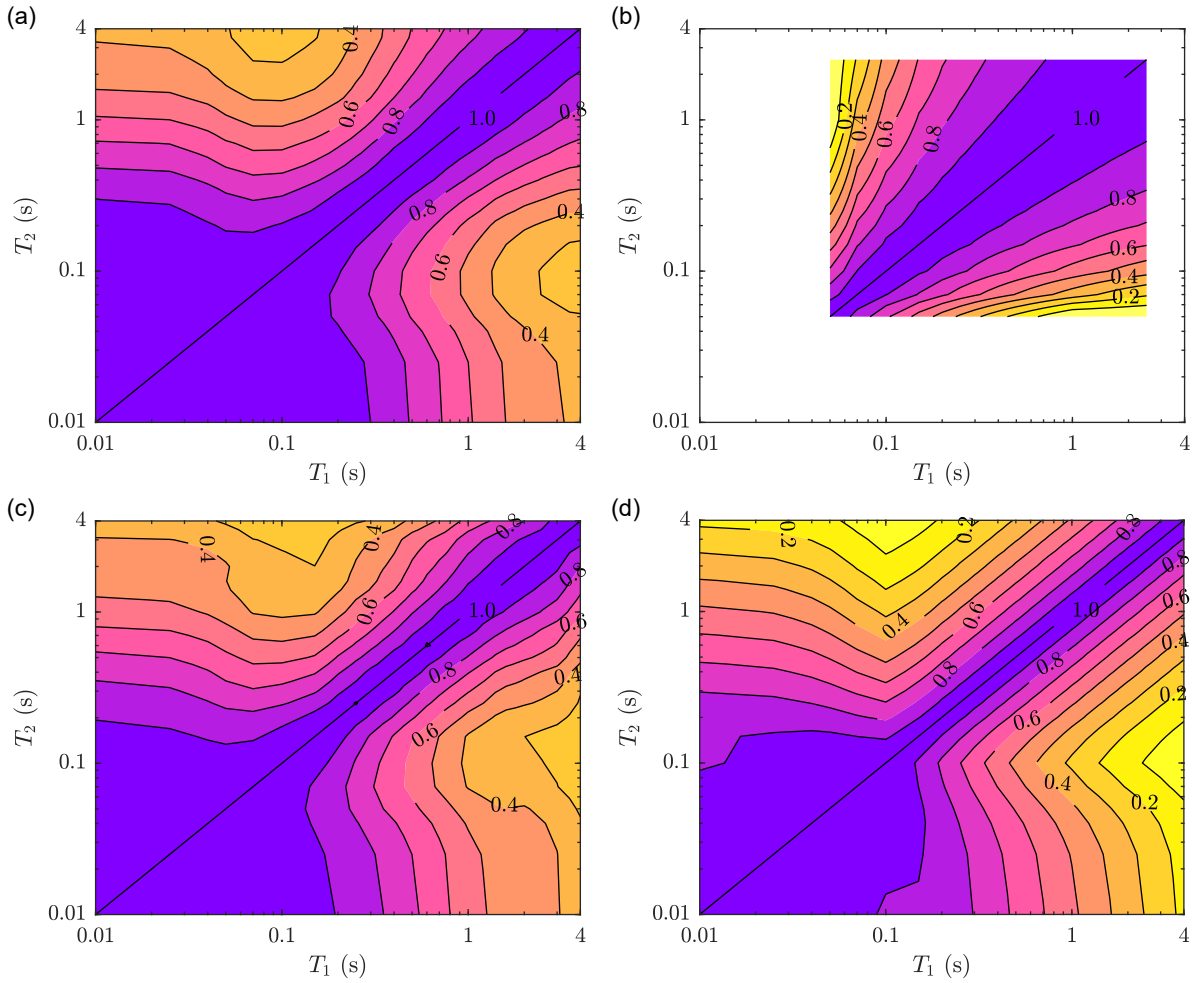

FIGURE 6 Contours of empirical PSA-PSA correlation coefficients as a function of T_1 and T_2 (ie, period pairs ranging 0.01 s and 4 s): (a) observations in the dataset considered; (b) model of Cimellaro (2013)[30] for Europe; (c) models of Akkar et al. (2014)[31] for Europe and the Middle East; (d) models of Baker and Jayaram (2008)[26] for worldwide shallow crustal regions. The color version of this figure is available only in the electronic edition.

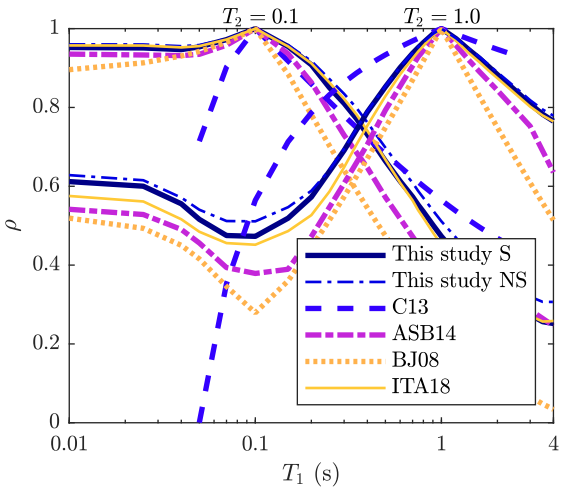

FIGURE 7 Empirical PSA-PSA correlation coefficients at two representative periods (ie, $T_2 = 0.1$ s and 1.0 s) versus T_1 ranging from 0.01 s and 4 s, in comparison of cross-IM correlation models applicable to Italy. The color version of this figure is available only in the electronic edition.

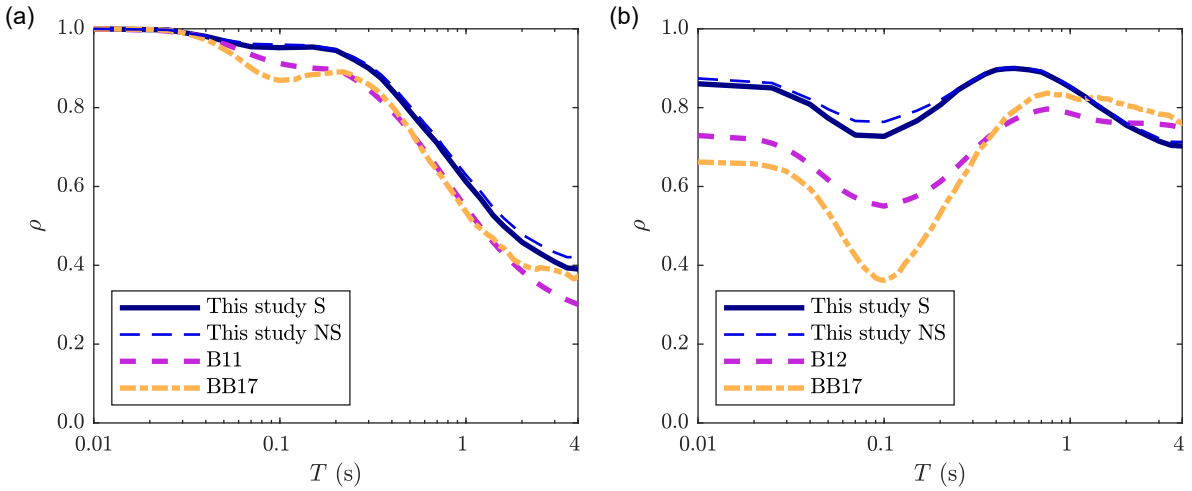

FIGURE 8 Empirical correlation coefficients for (a) PGA-PSA, (b) PGV-PSA versus T ranging from 0.01 s and 4 s, in comparison of cross-IM correlation models applicable to Italy. The color version of this figure is available only in the electronic edition.

this study and those computed from the ITA18 model are less than 0.5 (5%) for most period pairs, which seems to confirm the findings of Baker and Cornell[32] and Baker and Jayaram[26] that the GMM functional forms have little impact on correlation estimates (It is worth noting that ITA18 uses a slightly more complex functional form than the one used in this study).

The empirical correlation coefficients computed from the GMM without spatial correlation are also presented in Figure 7. Interestingly, Figure 7 shows that accounting for the spatial correlation in the GMM estimation has a negligible effect on the subsequent cross-IM correlation analysis, at least for the considered ground-motion IMs. As pointed out above, fitting a GMM without spatial correlation to the spatially correlated data results in an overestimation of the interevent standard deviation and an underestimation of the intraevent standard deviation; both these quantities enter in the definition of the IM correlation (Eq. 16). However, the differences in those quantities between the model with spatial correlation and that without spatial correlation are less than 10% for most of the spectral ordinates considered here, reaching about 15-20% in the case of PGA (e.g., Table 4) - similar results can be found in Jayaram and Baker[24]. On the other hand, these differences can become much larger when the correlation in the underlying data becomes higher (i.e., higher range parameter h; see for instance Ming et al.[6] for a detailed analysis on this aspect). Hence, one should not expect a significant bias in the existing cross-IM correlation model (based on GMM estimated without accounting for the spatial correlation), at least for the IM considered here.

The empirical PGA-PSA and PGV-PSA correlation coefficients are shown in Figure 8. The results are compared to the cross-IM correlation models in Table 2. As shown in Figure 8, the PGA-PSA and PGV-PSA correlations are similar to the considered studies, though the derived correlation coefficients are slightly higher than the reference models. Furthermore, the empirical PGA-PGV correlation coefficient is 0.861 in this study, which, again, is slightly higher than 0.733 obtained in Bradley[28]. The empirical correlation coefficients computed from the GMM without spatial correlation are also presented in Figure 8, confirming the above findings for the cross-PSA correlations.

These results show that the correlations observed in this study are generally higher (in terms of absolute value) than the considered models, which implies different features in the Italian data from that in the global dataset and may be possibly due to the poor representation of normal fault events in NGA-West2 dataset (19% normal fault events and 7% of total records)[50].

4.3 | The cross-IM correlation models

The results in the previous section show that there is a need for correlation models specifically calibrated based on the Italian data. In this section, a set of analytical correlation models between the selected IMs is developed. Following Baker and Jayaram[26],

the PSA-PSA correlation model is proposed as follows,

$$\text{if } T_{\max} \leq 0.1,\ \widetilde{\rho} = C_2 = 1 - 0.0617\left(1 - \frac{1}{1+\exp(100T_{\max}-5)}\right)\left(\frac{T_{\max}-T_{\min}}{T_{\max}-0.0099}\right); \tag{19}$$

$$\text{else if } T_{\min} > 0.1,\ \widetilde{\rho} = C_1 = 1 - \cos\left[\frac{\pi}{2} - 0.2351\ \ln(T_{\max}/T_{\min})\right]; \tag{20}$$

$$\text{else if } T_{\max} \leq 0.2,\ \widetilde{\rho} = \min(C_2, C_3); \tag{21}$$

$$\text{else } \widetilde{\rho} = C_3 = C_1 + 0.3131(\sqrt{C_1} - C_1)\left[1 + \cos\left(\frac{\pi T_{\min}}{0.1}\right)\right]. \tag{22}$$

where $T_{\max} = \max(T_1, T_2)$, $T_{\min} = \min(T_1, T_2)$.

Following Bradley[27,28], the analytical correlation models between PGA/PGV and structural period T are as follows,

$$\widetilde{\rho} = \frac{(\phi_1+\phi_2)}{2} - \frac{(\phi_1-\phi_2)}{2}\tanh\left[\phi_4 \ln\left(\frac{T}{\phi_3}\right)\right] \quad \text{for } t_{n-1} \leq T < t_n. \tag{23}$$

where the parameters ϕ_n are shown in Table 5.

It is worth noting that, as also discussed in Baker and Jayaram[26], there is no physical interpretation of the proposed functional forms in equations (19) to (23), which is only a fitting of the observed data and therefore should not be extrapolated.

The analytical PSA-PSA, PGA-PSA, and PGV-PSA correlation models are compared with the considered studies, as shown in Figure 9 and 10. These proposed correlation models are consistent with the empirical correlations observed in the Italian data. Moreover it accounts for the features observed in the Italian data that is not well captured in the considered studies.

TABLE 5 The estimated parameters in equation (23).

IMs	n	t_n	ϕ_1	ϕ_2	ϕ_3	ϕ_4
	0	0.01	-	-	-	-
PGA	1	0.2	1.000	0.950	0.045	2.225
	2	4	1.000	0.344	0.783	0.824
	0	0.01	-	-	-	-
PGV	1	0.1	0.859	0.722	0.045	2.533
	2	0.5	0.711	0.912	0.203	1.681
	3	4	0.917	0.686	1.450	1.306

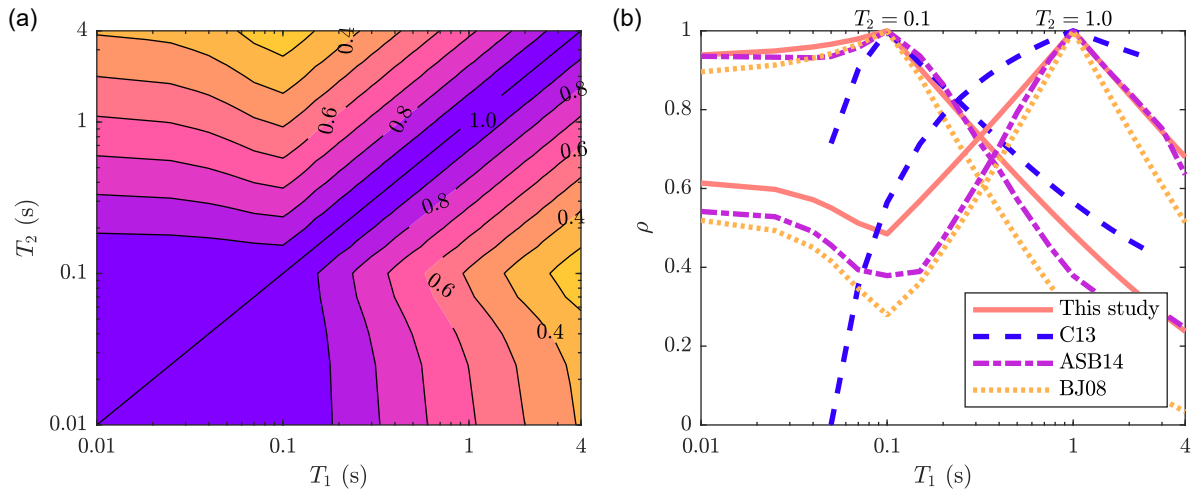

FIGURE 9 (a) Contour of analytical PSA-PSA correlation model at multiple period pairs ranging from 0.01 s to 4 s; (b) analytical PSA correlation model at two representative periods (ie, $T_2 = 0.1$ s and 1.0 s) versus T_1 ranging from 0.01 s and 4 s, in comparison of cross-IM correlation models applicable to Italy. The color version of this figure is available only in the electronic edition.

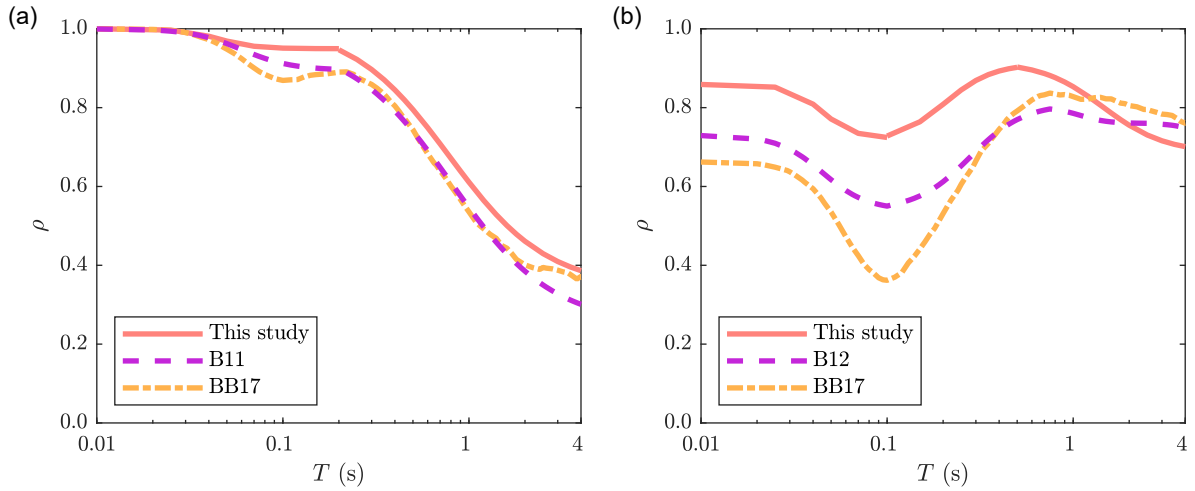

FIGURE 10 Analytical correlation models for (a) PGA-PSA, (b) PGV-PSA versus T ranging from 0.01 s and 4 s, in comparison of cross-IM correlation models applicable to Italy. The color version of this figure is available only in the electronic edition.

5 | DEPENDENCE OF CORRELATIONS ON MAGNITUDE AND DISTANCE

Following the study of Baker and Bradley[29], this section investigates the dependence of the cross-IM correlation on magnitude and distance by evaluating a set of empirical correlation coefficients computed from ground motions within varying magnitude and distance ranges and comparing them with the analytical models proposed in the previous section.

Figure 11 shows the empirical cross-IM correlation values for ground-motion records with $R_{JB} \leq 100$ km and $R_{JB} > 100$ km and magnitude $M_w \leq 4.5$ and $M_w \geq 6.0$ for several IM pairs compared with analytical correlation models. Regarding the PSA-PSA and PGA-PSA correlation, the empirical correlation coefficients for large magnitude (ie, $M_w \geq 6.0$) and small magnitude (ie, $M_w \leq 4.5$) are consistent with the analytical estimates, implying no significant magnitude dependence in these correlation values. These results are in line with the findings of Baker and Bradley[29].

Regarding the PGV-PSA correlation, the empirical correlation coefficients for ground motions from small magnitude events are generally consistent with the analytical estimates while those coming from large-magnitude events differ from the analytical ones, particularly at periods less than 0.5 s.

To further investigate the potential dependence on magnitude and distance, the cross-IM correlations are presented as a function of magnitude and distance of the input ground motions in Figure 12. The left panels in Figure 12 (a), (c) and (e) present the cross-IM correlations computed from ground motions with $R_{JB} \leq 100$ km and binned magnitude (± 0.3 unit around the target value). It is shown that there is no notable trend for PSA-PSA and PGA-PSA correlation against magnitude. Regarding the PGV-PSA correlations, the empirical correlation coefficients for small magnitude values are consistent with the analytical estimates, however, those corresponding to large magnitude values deviate from the analytical estimates. The correlation for PGV-PSA with short periods (ie, $T \leq 0.5$) tends to decrease and the correlation for PGV-PSA with long periods (ie, $T \geq 1.0$) tends to increase when magnitude increases, which is consistent with Figure 11 (c).

The right panels in Figure 12 (b), (d) and (f) show the cross-IM correlations computed from ground motions with $4.5 \leq M_w \leq 6$ (well-represented magnitude range in the considered dataset) and binned distance (± 15 km around the target value). It is shown that there is no notable trend for PSA-PSA and PGA-PSA correlation against distance. The PGV-PSA correlations for large distance (ie, $R_{JB} \geq 100$ km) are consistent with the analytical estimates while those for near-fault distance (ie, $R_{JB} \leq 100$ km) fluctuate around the analytical results.

In summary, it seems that the PSA-PSA and PGA-PSA correlations have no significant dependence on magnitude or distance, confirming the findings of Baker and Bradley[29]. However, there is some dependence of PGV-PSA correlation on magnitude and distance, particularly at periods less than 0.5 s.

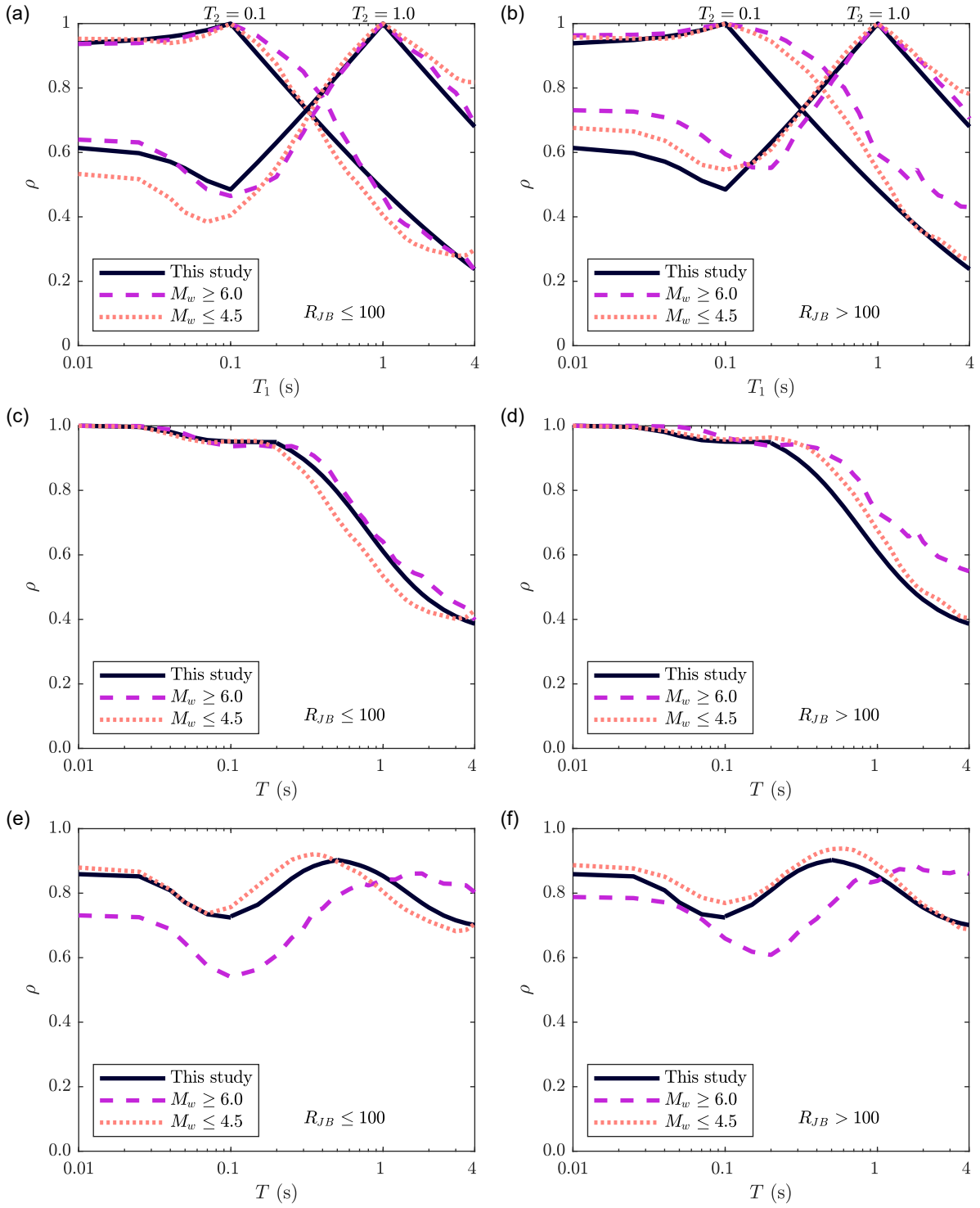

FIGURE 11 Empirical correlation coefficients for ground motions from $M_w \geq 6.0$ and $M_w \leq 4.5$ for (a) (b) PSA-PSA correlation at two representative periods, (c) (d) PGA-PSA correlation, and (e) (f) PGV-PSA correlation. Left panels are for $R_{JB} \leq 100$ km and right panels are for $R_{JB} > 100$ km. The color version of this figure is available only in the electronic edition.

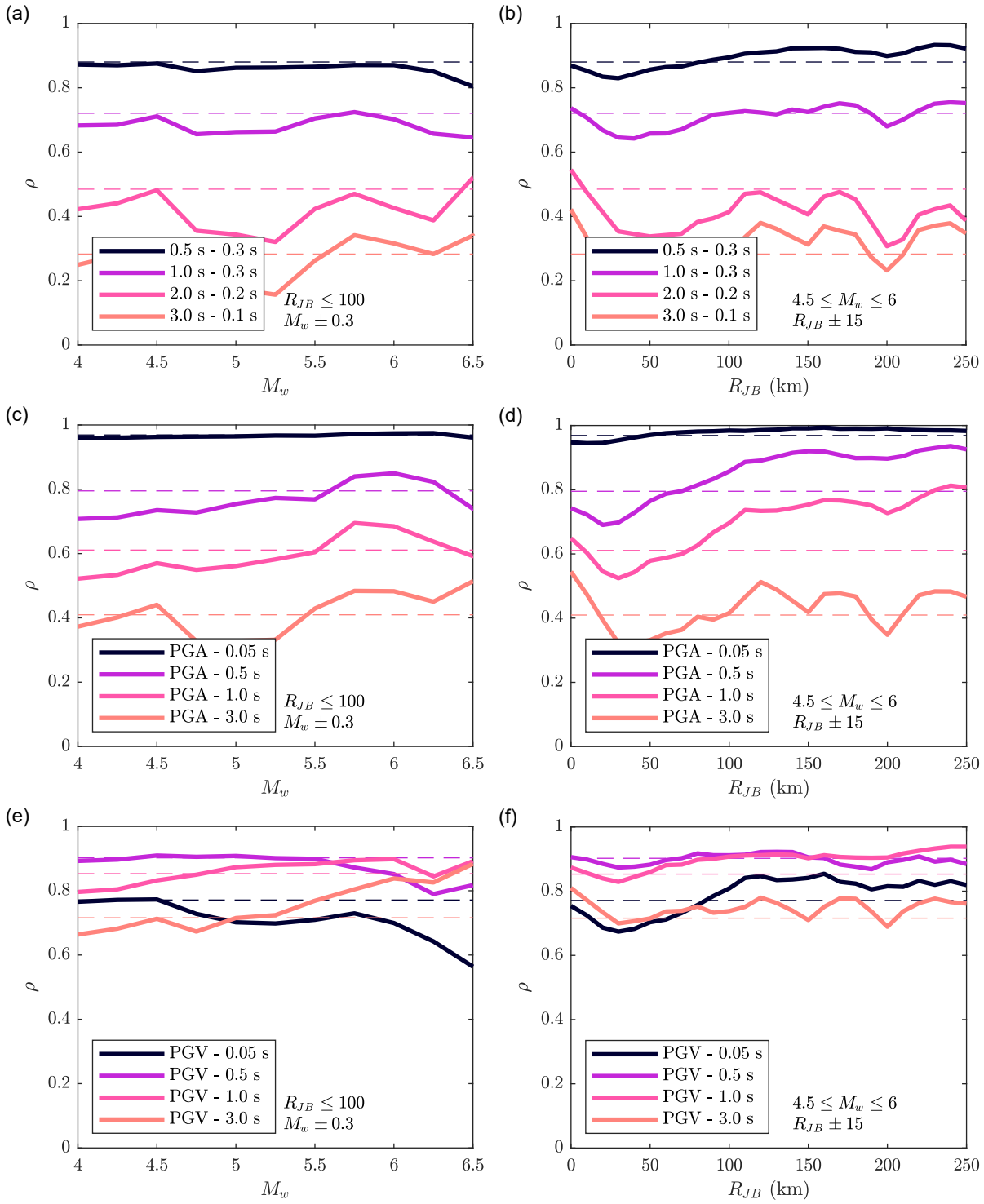

FIGURE 12 Cross-IM correlation coefficients for ground motions with a narrow range of magnitude (left panels) and distance (right panels) for (a) (b) PSA-PSA correlations, (c) (d) PGA-PSA correlations, (e) (f) PGV-PSA correlations. Solid lines are the empirical correlation coefficients and the dashed lines are the analytical correlation coefficients. The color version of this figure is available only in the electronic edition.

6 | CONCLUSIONS

This study has investigated the ground-motion IM correlation observed in Italian data. To this aim, this paper first used Italian strong-motion records to develop a new GMM with spatial correlation for 31 amplitude-based IMs, including PGA, PGV and 5%

damped elastic PSA at 29 periods ranging from 0.01 s to 4 s, by a recently-developed one-stage non-linear regression algorithm proposed by the authors. The median predictions of the proposed GMM is generally consistent with the existing GMMs for Europe and Italy. This study demonstrated that the inclusion of spatial correlation in GMM estimation reduces the interevent variance and increases the intraevent variance. The residual analysis showed that there is no bias in interevent residuals with respect to magnitude or in intraevent residuals with respect to distance, implying an overall good fitting of the proposed models to the Italian data. The estimated effective range of the spatial correlation function in this study was lower than that of the literature, which may be due to the use of the classical geostatistical method, which generally tends to overestimate the parameters in spatial correlation[6]. The total standard deviations in this study were slightly higher than the existing models in the literature, which may be partially because of the inclusion of spatial correlation and partially because of the larger dataset used in this study. Based on the newly-developed GMM, the empirical correlation between various IMs observed in the considered dataset were computed and compared to the existing correlation models, showing that the correlation features in the Italian data have not been adequately addressed by the literature. Finally, this study proposed a set of analytical correlation models between the selected IMs for the considered Italian ground-motion data. The PSA-PSA and PGA-PSA correlation have no significant dependence on magnitude and distance while the PGV-PSA correlation has notable dependence on large magnitude and short distance. The results of this study can be used to improve hazard/risk assessment exercises in Italy.

ACKNOWLEDGMENTS

This study is funded by the China Scholarships Council (grant number 201608440273). The authors are thankful to the two anonymous reviewers for their insightful remarks and suggestions to improve the manuscript. The authors thank Mr. Deyu Ming and Prof. Gareth W. Peters for their supports regarding the Scoring estimation approach. The strong-motion flatfile is obtained from the Engineering Strong-Motion (ESM) database http://esm.mi.ingv.it (last accessed May 2018). The Scoring estimation approach are implemented in MATLAB v.R2018a and the code is available at (GitHub link is not available yet).

APPENDIX

A THE EMPIRICAL CROSS-IM CORRELATION COEFFICIENTS

TABLE A1 Empirical cross-IM correlation coefficients (Part 1).

ρ	PGA	PGV	0.010	0.025	0.040	0.050	0.070	0.100	0.150	0.200	0.250	0.300
PGA	1	0.860894	0.999983	0.997196	0.980698	0.969658	0.954503	0.952140	0.953778	0.945317	0.922043	0.900011
PGV	0.860894	1	0.860520	0.850151	0.808272	0.773502	0.730389	0.727067	0.766467	0.806290	0.845147	0.867540
0.010	0.999983	0.860520	1	0.997471	0.981315	0.970192	0.954769	0.952108	0.953474	0.944961	0.921706	0.899541
0.025	0.997196	0.850151	0.997471	1	0.988191	0.976773	0.958246	0.950924	0.947554	0.937017	0.912256	0.888696
0.040	0.980698	0.808272	0.981315	0.988191	1	0.990737	0.966950	0.946736	0.927098	0.906982	0.875209	0.846655
0.050	0.969658	0.773502	0.970192	0.976773	0.990737	1	0.980684	0.953760	0.920268	0.890561	0.849575	0.818170
0.070	0.954503	0.730389	0.954769	0.958246	0.966950	0.980684	1	0.972128	0.925768	0.883135	0.830782	0.795033
0.100	0.952140	0.727067	0.952108	0.950924	0.946736	0.953760	0.972128	1	0.954596	0.908248	0.850426	0.810324
0.150	0.953778	0.766467	0.953474	0.947554	0.927098	0.920268	0.925768	0.954596	1	0.958216	0.907854	0.868890
0.200	0.945317	0.806290	0.944961	0.937017	0.906982	0.890561	0.883135	0.908248	0.958216	1	0.961093	0.924247
0.250	0.922043	0.845147	0.921706	0.912256	0.875209	0.849575	0.830782	0.850426	0.907854	0.961093	1	0.970605
0.300	0.900011	0.867540	0.899541	0.888696	0.846655	0.818170	0.795033	0.810324	0.868890	0.924247	0.970605	1
0.350	0.874693	0.885360	0.874164	0.862534	0.817279	0.785963	0.759320	0.771404	0.829313	0.886762	0.935831	0.974345
0.400	0.844783	0.895832	0.844228	0.831946	0.784898	0.751232	0.721092	0.731505	0.788674	0.846787	0.899555	0.941715
0.450	0.816778	0.898624	0.816203	0.803727	0.756126	0.720878	0.687522	0.695849	0.752959	0.812557	0.867572	0.912129
0.500	0.790233	0.899610	0.789641	0.776985	0.728954	0.692507	0.657986	0.664175	0.720073	0.779741	0.837014	0.884649
0.600	0.745661	0.896019	0.745061	0.732334	0.684449	0.646856	0.610146	0.613028	0.666749	0.725253	0.784671	0.835083
0.700	0.709850	0.890368	0.709268	0.697203	0.650546	0.611734	0.572709	0.573452	0.624230	0.681359	0.742451	0.794083
0.750	0.689572	0.883600	0.688984	0.676925	0.630753	0.591815	0.552559	0.552693	0.602393	0.658060	0.719584	0.771756
0.800	0.672765	0.876883	0.672178	0.660230	0.614685	0.575690	0.536037	0.535424	0.583602	0.638324	0.700187	0.753064
0.900	0.640651	0.864202	0.640074	0.628113	0.582849	0.543549	0.503114	0.501891	0.549162	0.603392	0.667008	0.720113
1.000	0.612437	0.851573	0.611878	0.600198	0.555536	0.516106	0.475051	0.472959	0.519021	0.572652	0.637619	0.691076
1.200	0.568656	0.827989	0.568163	0.557279	0.514211	0.474569	0.432384	0.429655	0.473470	0.525640	0.590017	0.643341
1.400	0.526700	0.804427	0.526231	0.515892	0.474228	0.434687	0.390828	0.386805	0.428454	0.481065	0.546173	0.600450
1.600	0.498941	0.786983	0.498505	0.488576	0.448198	0.408927	0.363797	0.359558	0.399894	0.452825	0.518727	0.572408
1.800	0.478026	0.770769	0.477592	0.467906	0.428489	0.389723	0.344507	0.340332	0.380100	0.432506	0.497906	0.550818
2.000	0.458779	0.755716	0.458327	0.448613	0.409290	0.370861	0.325403	0.320932	0.361450	0.413856	0.478975	0.531950
2.500	0.430386	0.732758	0.429936	0.420054	0.380969	0.343637	0.297543	0.294619	0.334461	0.386165	0.450637	0.502763
3.000	0.408848	0.714882	0.408458	0.399040	0.361203	0.323801	0.276640	0.273993	0.313221	0.363944	0.428458	0.478633
3.500	0.393311	0.704214	0.392972	0.383909	0.346628	0.308787	0.259794	0.256443	0.295320	0.345929	0.410938	0.461305
4.000	0.390552	0.702563	0.390274	0.381530	0.344539	0.306008	0.255548	0.251767	0.291055	0.341969	0.408215	0.458117

TABLE A2 Empirical cross-IM correlation coefficients (Part 2).

ρ	0.350	0.400	0.450	0.500	0.600	0.700	0.750	0.800	0.900	1.000	1.200	1.400	1.600
PGA	0.874693	0.844783	0.816778	0.790233	0.745661	0.709850	0.689572	0.672765	0.640651	0.612437	0.568656	0.526700	0.498941
PGV	0.885360	0.895832	0.898624	0.899610	0.896019	0.890368	0.883600	0.876883	0.864202	0.851573	0.827989	0.804427	0.786983
0.010	0.874164	0.844228	0.816203	0.789641	0.745061	0.709268	0.688984	0.672178	0.640074	0.611878	0.568163	0.526231	0.498505
0.025	0.862534	0.831946	0.803727	0.776985	0.732334	0.697203	0.676925	0.660230	0.628113	0.600198	0.557279	0.515892	0.488576
0.040	0.817279	0.784898	0.756126	0.728954	0.684449	0.650546	0.630753	0.614685	0.582849	0.555536	0.514211	0.474228	0.448198
0.050	0.785963	0.751232	0.720878	0.692507	0.646856	0.611734	0.591815	0.575690	0.543549	0.516106	0.474569	0.434687	0.408927
0.070	0.759320	0.721092	0.687522	0.657986	0.610146	0.572709	0.552559	0.536037	0.503114	0.475051	0.432384	0.390828	0.363797
0.100	0.771404	0.731505	0.695849	0.664175	0.613028	0.573452	0.552693	0.535424	0.501891	0.472959	0.429655	0.386805	0.359558
0.150	0.829313	0.788674	0.752959	0.720073	0.666749	0.624230	0.602393	0.583602	0.549162	0.519021	0.473470	0.428454	0.399894
0.200	0.886762	0.846787	0.812557	0.779741	0.725253	0.681359	0.658060	0.638324	0.603392	0.572652	0.525640	0.481065	0.452825
0.250	0.935831	0.899555	0.867572	0.837014	0.784671	0.742451	0.719584	0.700187	0.667008	0.637619	0.590017	0.546173	0.518727
0.300	0.974345	0.941715	0.912129	0.884649	0.835083	0.794083	0.771756	0.753064	0.720113	0.691076	0.643341	0.600450	0.572408
0.350	1	0.977781	0.952176	0.927241	0.882105	0.842504	0.821285	0.803334	0.772023	0.743333	0.696277	0.653610	0.625032
0.400	0.977781	1	0.982615	0.960383	0.920073	0.882320	0.862245	0.844878	0.815537	0.788477	0.742673	0.700725	0.671659
0.450	0.952176	0.982615	1	0.984704	0.947116	0.911658	0.892798	0.876160	0.848022	0.822043	0.778396	0.737234	0.708849
0.500	0.927241	0.960383	0.984704	1	0.970001	0.936975	0.919659	0.903990	0.877342	0.852223	0.809843	0.770477	0.742885
0.600	0.882105	0.920073	0.947116	0.970001	1	0.974839	0.960165	0.947142	0.923545	0.901140	0.861962	0.824550	0.798078
0.700	0.842504	0.882320	0.911658	0.936975	0.974839	1	0.991707	0.979841	0.957897	0.937328	0.902000	0.866732	0.840952
0.750	0.821285	0.862245	0.892798	0.919659	0.960165	0.991707	1	0.992700	0.971400	0.951878	0.918089	0.884683	0.859260
0.800	0.803334	0.844878	0.876160	0.903990	0.947142	0.979841	0.992700	1	0.983284	0.964475	0.932010	0.900539	0.875930
0.900	0.772023	0.815537	0.848022	0.877342	0.923545	0.957897	0.971400	0.983284	1	0.986162	0.955618	0.926855	0.903550
1.000	0.743333	0.788477	0.822043	0.852223	0.901140	0.937328	0.951878	0.964475	0.986162	1	0.974313	0.947008	0.924976
1.200	0.696277	0.742673	0.778396	0.809843	0.861962	0.902000	0.918089	0.932010	0.955618	0.974313	1	0.977895	0.957735
1.400	0.653610	0.700725	0.737234	0.770477	0.824550	0.866732	0.884683	0.900539	0.926855	0.947008	0.977895	1	0.983427
1.600	0.625032	0.671659	0.708849	0.742885	0.798078	0.840952	0.859260	0.875930	0.903550	0.924976	0.957735	0.983427	1
1.800	0.602803	0.648014	0.684741	0.718842	0.774108	0.817689	0.836289	0.853219	0.881157	0.903111	0.936916	0.963898	0.985595
2.000	0.583560	0.627445	0.663646	0.697294	0.752456	0.796160	0.814819	0.831817	0.860428	0.883279	0.917866	0.946456	0.968538
2.500	0.550309	0.591622	0.626656	0.659850	0.713128	0.755325	0.773073	0.789931	0.819567	0.842803	0.878648	0.909132	0.931692
3.000	0.523998	0.565748	0.600114	0.631565	0.682831	0.723164	0.739900	0.755857	0.785507	0.808930	0.845923	0.877681	0.899945
3.500	0.505557	0.547319	0.580970	0.611222	0.660993	0.699556	0.715673	0.730348	0.759708	0.782786	0.819939	0.853017	0.874794
4.000	0.501379	0.542346	0.574660	0.603735	0.650288	0.685977	0.700930	0.714511	0.742690	0.765196	0.801216	0.834034	0.855353

TABLE A3 Empirical cross-IM correlation coefficients (Part 3).

ρ	1.800	2.000	2.500	3.000	3.500	4.000
PGA	0.478026	0.458779	0.430386	0.408848	0.393311	0.390552
PGV	0.770769	0.755716	0.732758	0.714882	0.704214	0.702563
0.010	0.477592	0.458327	0.429936	0.408458	0.392972	0.390274
0.025	0.467906	0.448613	0.420054	0.399040	0.383909	0.381530
0.040	0.428489	0.409290	0.380969	0.361203	0.346628	0.344539
0.050	0.389723	0.370861	0.343637	0.323801	0.308787	0.306008
0.070	0.344507	0.325403	0.297543	0.276640	0.259794	0.255548
0.100	0.340332	0.320932	0.294619	0.273993	0.256443	0.251767
0.150	0.380100	0.361450	0.334461	0.313221	0.295320	0.291055
0.200	0.432506	0.413856	0.386165	0.363944	0.345929	0.341969
0.250	0.497906	0.478975	0.450637	0.428458	0.410938	0.408215
0.300	0.550818	0.531950	0.502763	0.478633	0.461305	0.458117
0.350	0.602803	0.583560	0.550309	0.523998	0.505557	0.501379
0.400	0.648014	0.627445	0.591622	0.565748	0.547319	0.542346
0.450	0.684741	0.663646	0.626656	0.600114	0.580970	0.574660
0.500	0.718842	0.697294	0.659850	0.631565	0.611222	0.603735
0.600	0.774108	0.752456	0.713128	0.682831	0.660993	0.650288
0.700	0.817689	0.796160	0.755325	0.723164	0.699556	0.685977
0.750	0.836289	0.814819	0.773073	0.739900	0.715673	0.700930
0.800	0.853219	0.831817	0.789931	0.755857	0.730348	0.714511
0.900	0.881157	0.860428	0.819567	0.785507	0.759708	0.742690
1.000	0.903111	0.883279	0.842803	0.808930	0.782786	0.765196
1.200	0.936916	0.917866	0.878648	0.845923	0.819939	0.801216
1.400	0.963898	0.946456	0.909132	0.877681	0.853017	0.834034
1.600	0.985595	0.968538	0.931692	0.899945	0.874794	0.855353
1.800	1	0.987761	0.950330	0.917715	0.892445	0.872729
2.000	0.987761	1	0.968384	0.936588	0.911255	0.891524
2.500	0.950330	0.968384	1	0.977222	0.954070	0.933579
3.000	0.917715	0.936588	0.977222	1	0.984227	0.964994
3.500	0.892445	0.911255	0.954070	0.984227	1	0.987600
4.000	0.872729	0.891524	0.933579	0.964994	0.987600	1

References

1. Park J, Bazzurro P, Baker JW. Modeling spatial correlation of ground motion Intensity Measures for regional seismic hazard and portfolio loss estimation. In: Kanda J, Takada T, Furuta H., eds. *Applications of Statistics and Probability in Civil Engineering*London, United Kingdom: Taylor and Francis Group. 2007 (pp. 1–8).

2. Jayaram N, Baker JW. Correlation model for spatially distributed ground-motion intensities. *Earthq Eng Struct Dynam* 2009; 38(15): 1687–1708.

3. Weatherill GA, Silva V, Crowley H, Bazzurro P. Exploring the impact of spatial correlations and uncertainties for portfolio analysis in probabilistic seismic loss estimation. *Bull Earthq Eng* 2015; 13(4): 957–981. doi: 10.1007/s10518-015-9730-5

4. Bradley BA. A generalized conditional intensity measure approach and holistic ground-motion selection. *Earthq Eng Struct Dynam* 2010; 39(12): 1321–1342. doi: 10.1002/eqe.995

5. Lin T, Baker JW. Conditional Spectra. In: Beer M, Kougioumtzoglou IA, Patelli E, Au SK., eds. *Encyclopedia of Earthquake Engineering*Heidelberg, Germany: Springer. 2015 (pp. 461–472)

6. Ming D, Huang C, Peters GW, Galasso C. An advanced estimation algorithm for ground-motion models with spatial correlation. *Bull Seismol Soc Am* 2019. doi: 10.1785/0120180215

7. Douglas J. Ground motion prediction equations 1964-2018. 2018. doi: 10.1017/CBO9781107415324.004

8. Ambraseys NN, Douglas J, Sarma SK, Smit PM. Equations for the estimation of strong ground motions from shallow crustal earthquakes using data from Europe and the middle east: Horizontal peak ground acceleration and spectral acceleration. *Bull Earthq Eng* 2005; 3(1): 1–53. doi: 10.1007/s10518-005-0183-0

9. Chiou BSJ, Youngs RR. An NGA model for the average horizontal component of peak ground motion and response spectra. *Earthq Spectra* 2008; 24(1): 173–215. doi: 10.1193/1.2894832

10. Akkar S, Bommer JJ. Empirical equations for the prediction of PGA, PGV, and spectral accelerations in Europe, the Mediterranean region, and the Middle East. *Seismological Research Letters* 2010; 81(2): 195–206.

11. Bindi D, Pacor F, Luzi L, et al. Ground motion prediction equations derived from the Italian strong motion database. *Bull Earthq Eng* 2011; 9(6): 1899–1920.

12. Akkar S, Sandıkkaya MA, Bommer JJ. Empirical ground-motion models for point- and extended-source crustal earthquake scenarios in Europe and the Middle East. *Bull Earthq Eng* 2014; 12(1): 359–387.

13. Akkar S, Sandıkkaya MA, Bommer JJ. Erratum to: Empirical ground-motion models for point- and extended-source crustal earthquake scenarios in Europe and the Middle East. *Bull Earthq Eng* 2014; 12(1): 389–390.

14. Chiou BSJ, Youngs RR. Update of the Chiou and Youngs NGA model for the average horizontal component of peak ground motion and response spectra. *Earthq Spectra* 2014; 30(3): 1117–1153. doi: 10.1193/072813EQS219M

15. Lanzano G, Luzi L, Pacor F, et al. A revised ground-motion prediction model for shallow crustal earthquakes in Italy. *Bull Seismol Soc Am* 2019. doi: 10.1785/0120180210

16. Lanzano G, Sgobba S, Luzi L, et al. The pan-European engineering strong motion (ESM) flatfile: Compilation criteria and data statistics. *Bull Earthq Eng* 2018. doi: 10.1007/s10518-018-0480-z

17. Abrahamson NA, Youngs RR. A stable algorithm for regression analyses using the random effects model. *Bull Seismol Soc Am* 1992; 82(1): 505–510.

18. Joyner WB, Boore DM. Methods for regression analysis of strong-motion data. *Bull Seismol Soc Am* 1993; 83(2): 469–487.

19. Bates D, Mächler M, Bolker BM, Walker SC. Fitting linear mixed-effects models using lme4. *J Stat Software* 2015; 67(1). doi: 10.18637/jss.v067.i01

20. Pinheiro JC, Bates D. *Mixed-Effects Models in S and S-PLUS*. Madison, Wisconsin: Springer . 2000.

21. Lanzano G, D'Amico M, Felicetta C, et al. Ground-motion prediction equations for region-specific probabilistic seismic-hazard analysis. *Bull Seismol Soc Am* 2016; 106(1): 73–92. doi: 10.1785/0120150096

22. Esposito S, Iervolino I. PGA and PGV spatial correlation models based on European multievent datasets. *Bull Seismol Soc Am* 2011; 101(5): 2532–2541. doi: 10.1785/0120110117

23. Esposito S, Iervolino I. Spatial correlation of spectral acceleration in European data. *Bull Seismol Soc Am* 2012; 102(6): 2781–2788.

24. Jayaram N, Baker JW. Considering spatial correlation in mixed-effects regression and the impact on ground-motion models. *Bull Seismol Soc Am* 2010; 100(6): 3295–3303.

25. Zimmerman DL, Michael S. Classical Geostatistical Methods. In: Gelfand AE, Diggle PJ, Fuentes M, Guttorp P., eds. *Handbook of Spatial Statistics*Boca Raton, Florida: CRC Press. 2010 (pp. 29–44).

26. Baker JW, Jayaram N. Correlation of spectral acceleration values from NGA ground motion models. *Earthq Spectra* 2008; 24(1): 299–317.

27. Bradley BA. Empirical correlation of PGA, spectral accelerations and spectrum intensities from active shallow crustal earthquakes. *Earthq Eng Struct Dynam* 2011; 40(15): 1707–1721.

28. Bradley BA. Empirical correlations between peak ground velocity and spectrum-based intensity measures. *Earthq Spectra* 2012; 28(1): 17–35.

29. Baker JW, Bradley BA. Intensity measure correlations observed in the NGA-West2 database, and dependence of correlations on rupture and site parameters. *Earthq Spectra* 2017; 33(1): 145–156.

30. Cimellaro GP. Correlation in spectral accelerations for earthquakes in Europe. *Earthq Eng Struct Dynam* 2013; 42(4): 623–633.

31. Akkar S, Sandıkkaya MA, Ay BÖ. Compatible ground-motion prediction equations for damping scaling factors and vertical-to-horizontal spectral amplitude ratios for the broader Europe region. *Bull Earthq Eng* 2014; 12(1): 517–547.

32. Baker JW, Cornell CA. Correlation of response spectral values for multicomponent ground motions. *Bull Seismol Soc Am* 2006; 96(1): 215–227. doi: 10.1785/0120050060

33. Scasserra G, Stewart JP, Bazzurro P, Lanzo G, Mollaioli F. A comparison of NGA ground-motion prediction equations to Italian data. *Bull Seismol Soc Am* 2009; 99(5): 2961–2978. doi: 10.1785/0120080133

34. Kotha SR, Bindi D, Cotton F. Partially non-ergodic region specific GMPE for Europe and Middle-East. *Bull Earthq Eng* 2016; 14(4): 1245–1263.

35. Boore DM, Stewart JP, Seyhan E, Atkinson GM. NGA-West2 equations for predicting PGA, PGV, and 5% damped PSA for shallow crustal earthquakes. *Earthq Spectra* 2014; 30(3): 1057–1085.

36. Rasmussen CE, Williams CKI. *Gaussian Processes for Machine Learning*. Cambridge, Massachusetts: MIT Press . 2006.

37. Boore DM. Orientation-independent, nongeometric-mean measures of seismic intensity from two horizontal components of motion. *Bull Seismol Soc Am* 2010; 100(4): 1830–1835. doi: 10.1785/0120090400

38. Huang C, Galasso C. A comparison of NGA-West2 ground-motion models to recent Chinese data. *Soil Dynam Earthq Eng* 2019. (under review).

39. Fisher RA. Theory of statistical estimation. *Math Proc Camb Phil Soc* 1925; 22(5): 700–725.

40. Goda K, Hong HP. Spatial correlation of peak ground motions and response spectra. *Bull Seismol Soc Am* 2008; 98(1): 354–365. doi: 10.1785/0120070078

41. Arroyo D, Ordaz M. Multivariate bayesian regression analysis applied to ground-motion prediction equations, Part 2 : Numerical example with actual data. *Bull Seismol Soc Am* 2010; 100(4): 1568–1577.

42. Stucchi M, Meletti C, Montaldo V, Crowley H, Calvi GM, Boschi E. Seismic hazard assessment (2003-2009) for the Italian building code. *Bull Seismol Soc Am* 2011; 101(4): 1885–1911. doi: 10.1785/0120100130

43. CEN . *Eurocode 8: Design of structures for earthquake resistance, Part 1: General rules, seismic actions and rules for buildings, EN 1998-1*. Brussels: European Committee for Standardization(CEN) . 2004.

44. Zimmaro P, Scasserra G, Stewart J, Kishida T. Strong ground motion characteristics from 2016 central Italy earthquake sequence. *Earthq Spectra* 2018; 34(4): 1611–1637.

45. Akaike H. A new look at the statistical model identification. *IEEE Transactions on Automatic Control* 1974; 19(6): 716–723.

46. Schwarz G. Estimating the dimension of a model. *The Annals of Statistics* 1978; 6(2): 461–464.

47. Bommer JJ, Douglas J, Strasser FO. Style-of-faulting in ground-motion prediction equations. *Bull Earthq Eng* 2003; 1(2): 171–203. doi: 10.1023/A:1026323123154

48. Chiou BSJ, Darragh R, Gregor N, Silva WJ. NGA project strong-motion database. *Earthq Spectra* 2008; 24(1): 23–44. doi: 10.1193/1.2894831

49. Akkar S, Sandıkkaya MA, Şenyurt M, et al. Reference database for seismic ground-motion in Europe (RESORCE). *Bull Earthq Eng* 2014; 12(1): 311–339.

50. Ancheta TD, Darragh RB, Stewart JP, et al. NGA-West2 database. *Earthq Spectra* 2014; 30(3): 989–1005.